ISSN 0016-7029, Geochemistry International, 2009, Vol. 47, No. 5, pp. 425–453. © Pleiades Publishing, Ltd., 2009.
Original Russian Text © A.A. Ariskin, E.G. Konnikov, L.V. Danyushevsky, E.V. Kislov, G.S. Nikolaev, D.A. Orsoev, G.S. Barmina, K.A. Bychkov, 2009, published in Geokhimiya, 2009, No. 5, pp. 451–480.

The Dovyren Intrusive Complex: Problems of Petrology and Ni Sulfide Mineralization

A. A. Ariskin [a], E. G. Konnikov [b], L. V. Danyushevsky [c], E. V. Kislov [d], G. S. Nikolaev [a], D. A. Orsoev [d], G. S. Barmina [a], and K. A. Bychkov [a, c]

[a] *Vernadsky Institute of Geochemistry and Analytical Chemistry, Russian Academy of Sciences, ul. Kosygina 19, Moscow, 119991 Russia*
e-mail: ariskin@rambler.ru

[b] *Institute of Experimental Mineralogy, Russian Academy of Sciences, ul. Institutskaya 4, Chernogolovka, Moscow oblast, 142432 Russia*

[c] *Centre for Ore Deposit Research (CODES), University of Tasmania, Hobart, Australia*

[d] *Geological Institute, Siberian Branch, Russian Academy of Sciences, ul. Sakh'yanovoi 6, Ulan-Ude, 670047 Russia*

Received October 30, 2009

Abstract—This paper presents a review of petrological–geochemical studies at the Yoko-Dovyren Massif with an emphasis on relations between parameters of the parental magma, a model for the genesis of the lower contact zone, and the nature of Ni sulfide ore mineralization, including the evaluation of the possible ore potential. Arguments are presented in support of the conclusion that the Dovyren magma brought much intratelluric olivine of the composition $Fo_{85–87}$into the chamber, and the composition of the initial melt corresponded to gabbronorite or moderately magnesian basite with no more than 10 wt % MgO. The probable temperature of the parental magma was approximately 1200–1250°C, and the sulfur solubility did not exceed 0.10–0.12 wt % (P = 1 kbar, WM buffer). The comparison of this estimate with the average S contents in the bottom plagioperidotites (0.12 ± 0.06 wt %) indicates that the initial magma was saturated with a sulfide phase. For the first time the problem of the composition of contaminated dunites was formulated (these rocks occur in the Layered Series and contain more magnesian olivine $Fo_{87–92}$). The reason for the increase in the mg# of olivine is thought to be the partial melting and compaction of the original cumulates due to the infiltration of intercumulus melt enriched in volatile components. The volatiles were presumably provided by the thermal decomposition of carbonate xenoliths, a process that resulted in an increase in the CO_2 pressure and the transfer of calcite–magnesite components of carbonates into the melt. This follows from (1) the occurrence of magnesian skarn developing after carbonates, (2) high CaO contents in olivine form the contaminated dunite, (3) the appearance of olivine-bearing pyroxenites and wehrlites in the upper part of the dunite zone, (4) correlation between the olivine and chromite composition in the contaminated and uncontaminated dunites, (5) broad variations in the oxygen isotopic composition of olivine and plagioclase from rocks of the Layered Series, (6) experimental data on the dissolution of carbonates in alkali basalt melts, and (7) analogies with isotopic–geochemical characteristics of rocks from the Jinchuan ultramafic complex. Petrological implications of the interpretation of the Dovyren chamber are discussed with reference to closed and flow-through (during an initial stage) magmatic systems. A petrological–geological model is proposed for the genesis of the Synnyr–Dovyren volcanic–plutonic complex and related Ni sulfide ore mineralization. The potential resources of Cu–Ni sulfide ores in the plagioperidotites are evaluated with regard to the still-unexposed part of the massif.

DOI: 10.1134/S0016702909050012

INTRODUCTION

Along with the broadly known Cu–Ni–PGE sulfide mineral deposits in the Noril'sk region, folded structures surrounding the Siberian Platform host other promising deposits of the same metallogenic type, which were discovered in the early 1960s but are still relatively poorly explored. These are layered intrusions and complexes of mafic–ultramafic composition, such as the Kingash Massif in the Western Sayan and Dovyren plutons and the Chaya and Nyurundukan massifs in the northwestern Baikal area, the Chinei Intrusion in the northern Transbaikalye, the Luchan Massif in the Stanovoi Range, and a number of smaller bodies. These intrusions are accompanied by ore mineralization or are potentially metalliferous and attract a lot of interest of geological organizations and mining companies in the context of incrementing the resources of sulfide ores and precious metals in eastern Siberia. Attention was recently focused on the geological–geochemical mapping of intrusive basites and ultrabasites, and a new exploration cycle was launched with the evaluation and reevaluation of the related resources of ores and metals. In this situation more stringent requirements are imposed upon the utilization of available geological potential, the application of state-of-the-art technolo-

gies, and the development of newly developed and scientifically justified criteria for the exploration and evaluation of Ni sulfide ore resources. These problems cannot be solved based on the results of a geological survey alone (with the application of traditional geochemical and geophysical methods). An ever higher priority is thereby given to the analysis and qualified utilization of genetic information on the nature of sulfide-forming processes, including data on the thermodynamic conditions under which the sulfide phases were formed, the dynamics of their transfer and redistribution (segregation) in magmatic melts, and conditions of their concentration in the course of magmatic evolution.

Modern petrological models of processes generating Ni sulfide ore mineralization are underlain by data on magmatic complexes and volcanic suites that characterize the major types of the petrotectonic provinces of the Earth [1, 2]. The synthesis of these materials led to the conclusion that the genesis of most Cu–Ni deposits was related to mafic magmatism during rifting at the margins of continental cratons. Further support for this is provided by the results obtained on classic mineralized intrusions at Labrador (Voisey's Bay), anorthosite–troctolite massifs of the Duluth Complex in Minnesota, comagmatic suites at Pechenga in northern Russia, and magnesian basalts at Jinchuan in northern China. Important studies were conducted on volcanic–plutonic associations in the northwestern Siberian Platform. The results obtained on fertile and barren intrusions in the Talnakh group of mineral deposits and data on the geochemistry of basalts of coeval associations made it possible to formulate the fundamentals of a basic geological–geochemical model for the genesis of Cu–Ni sulfide deposits [1–5]. In spite of certain differences between these petrological schemes, they imply that the ore-forming systems developed from a combination of a number of favorable factors, including (1) the presence of parental magmas containing at least ~100 ppm Ni, (2) the onset of sulfide–silicate immiscibility (usually triggered by contamination with crustal material), (2) the possibility of migration for the contaminated and hybrid basaltic magmas to upper crustal levels without significant loss of the sulfide phase, and (4) a certain mechanism of sulfide precipitation in the magmatic conduit or chamber [6–9]. The relative contribution of these processes to the origin of individual mineral deposits, the extent of sulfide concentration, and the corresponding signatures in the geochemistry of the comagmatic volcanics should be different. This highlights the necessity of systematizing data on the structures of intrusive complexes and the geochemical specifics of riftogenic volcanic associations that characterize various geological–tectonic regimes forming sulfide deposits during discrete stages of geological history. Thereby a more and more important role is played not only by analytical investigations and geochemical synthesis but also by new petrological approaches underlain by information on tiny inclusions in minerals [10, 11] and the application of modern numerical simulations for the crystallization differentiation of basite magmas [12, 13].

The integration of petrological and geochemical techniques in application to the genesis of Ni sulfide ore mineralization and the development of new prospecting guides for Cu–Ni–PGE ores cannot now be accomplished simultaneously for numerous intrusive and volcanic basites. It is very important to select reference volcano-plutonic associations comprising genetically interrelated layered massifs, hypabyssal bodies, and volcanic rocks that are characterized by diverse modes of occurrence of sulfides of magmatic and/or fluid–magmatic genesis. Such a reference complex should be characterized by unambiguous geological relations within a certain association, the availability of accessible and well exposed vertical sections (drill core), the good preservation of the rocks and minerals, and the presence of diverse types of sulfide mineralization. In Russia, one of the most suitable (along with the Norilsk province) provinces for the solution of such problems is the northern Baikal metallogenic province, which hosts the largest Kholodninskoe base-metal deposit [14, 15] and the Baikal'skoe Cu–Ni deposit with massive Cu–Ni sulfide ores at the bottom of the Yoko–Dovyren layered pluton [16]. This layered dunite–troctolite–gabbronorite–norite massif is now one of the most thoroughly examined intrusions in Russia and composes, together with the accompanying hypabyssal bodies of plagioclase lherzolites and gabbronorites, the Late Riphean Dovyren intrusive complex [17–25]. The rocks of this complex are thought to be comagmatic and roughly coeval with the volcanics of the Synnyr rift and likely compose a common genetic sequence of volcanic rocks and mafic–ultramafic rocks of a single Late Riphean Synnyr–Dovyren volcanic–plutonic complex (Fig. 1). There are good reasons to believe that the Dovyren pluton itself was formed in a thick magmatic chamber that belonged to a large-scale mantle–crustal magma-feeding system [20, 26]. Hence, many lines of evidence indicate that this volcanic–plutonic association is almost ideal for the detailed geochemical and petrological study of magmatic processes that generated sulfide mineralization in the course of the evolution of the Synnyr magmatic system in the southern margin of the Siberian craton in the Late Proterozoic.

Although the Dovyren intrusion was mapped in much detail and its composition has been studied for a long time, the petrological interpretation of its inner structure is ambiguous: the temperature evaluations and the composition of the parental Dovyren magma are disputable, and the differentiation of this magma was explained by various mechanisms [22, 27–29]. It is also uncertain as to how open or closed was the magmatic chamber and what role was played by the processes of the early crustal contamination of the parental magma before its injection into the chamber [30, 31], as well as

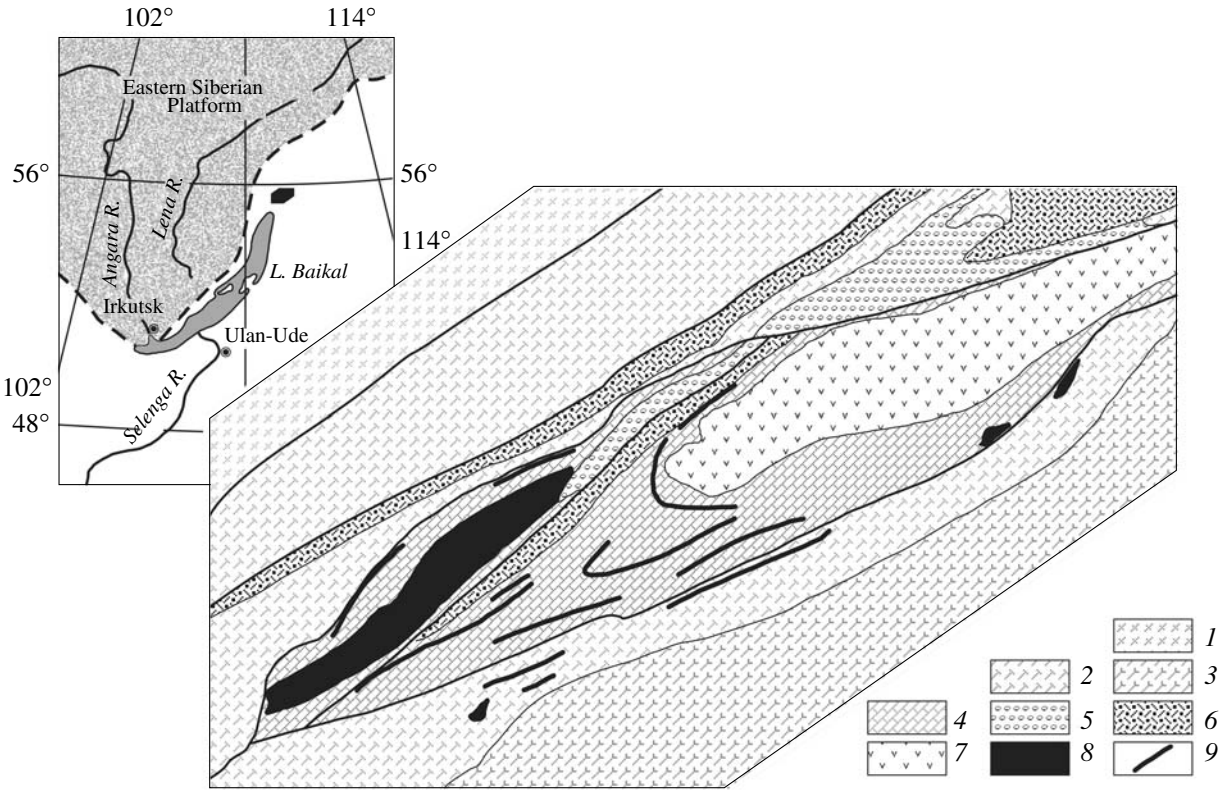

Fig. 1. Schematic geological map of the Synnyr–Dovyren volcano-plutonic association (based on [21, 34]).
(*1*) Chuya (Kutim) inlier of crystalline basement rocks (AR–PR_1); (*2*) terrigenous deposits of the Olokit trough; (*3*) island arc metavolcanics (R_2?); (*4–7*) rocks of the Synnyr rift (R_3–V): (*4*) carbonate–terrigenous–shale sediments, (*5*) Vendian conglomerates, (6) basalt–andesite–rhyolite Inyaptuk Formation, (*7*) andesites of the Synnyr Formation; (*8*, *9*) Dovyren intrusive complex: (*8*) Yoko–Dovyren pluton and ultramafic sills, (*9*) gabbronorite and gabbro-diabase sills. The inset shows the location of volcano-plutonic complexes in the folded structures surrounding the Siberian Platform (white).

the role of the assimilation of the host rocks during the emplacement of the intrusion [32, 33]. Other highly uncertain issues include the nature, reasons for, and scale of sulfide segregation in the bottom rocks of the Dovyren intrusion, including sills of plagioclase lherzolites and gabbronorites. The situation with the comagmatic nature of the Synnyr volcanics (*Inyaptukskaya* and *Synnyr* formations) is also largely uncertain. The conclusion about their possible genetic links with rocks of the Dovyren Complex is based mostly on geological evidence (Fig. 1). Practically all data available as of the present are contained in the not very voluminous monograph [17] and a few whole-rock analyses of the volcanics with a limited number of geochemical characteristics [21].

This publication presents a synthesis of this information and outlines avenues for the further study of the Yoko-Dovyren Massif with the use of modern petrological and geochemical methods. The results of these studies can be useful for the development of genetic models for various types of Ni sulfide mineralization related to mafite–ultramafite intrusions during the evolution of large magma feeding systems.

GEOLOGY OF THE DOVYREN COMPLEX

The Yoko–Dovyren Massif, its accompanying hypabyssal bodies, and the volcanic rocks of the Synnyr rift (Fig. 1) are thought to compose a single volcanic–plutonic association, which was formed in the Late Riphean in the southwestern part of the Olokit–Bodaibo trough [20, 34]. Geodynamic reconstructions suggest that this trough was produced in relation to the evolution of the Baikal–Patom paleobasin, which separated the Siberian craton and Baikal–Muya ensimatic island arc in the Proterozoic. The continental basement of the paleobasin is exposed at the surface in the Chuya and Chara inliers. A carbonate–terrigenous sequence many kilometers thick accumulated there in the Early Proterozoic and Riphean and was then metamorphosed to the greenschist and amphibolite facies. Collision processes in the margin of the Siberian craton in the Late Riphean were associated with the large-scale northeasterly (in modern coordinates) horizontal displacements of the terranes and the origin of the Synnyr rift structure approximately 150 km long and 12–15 km wide.

The deposits of the Synnyr rift trough are underlain by sand–shale–carbonate sediments of the *Dovyren*

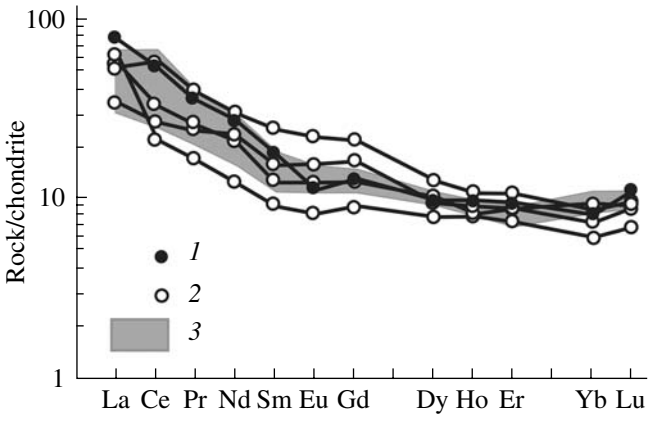

Fig. 2. Chondrite-normalized REE patterns for rocks of the Synnyr Formation and Yoko–Dovyren layered massif [21]. (*1*) Gabbro-diabase sill in the Ityka siltstone underlying the Synnyr volcanic rocks in Mount Soldat; (*2*) basaltic andesites and andesites of the Synnyr Formation; (*3*) granophyric gabbronorites of the upper vertical section of the Yoko–Dovyren Massif.

Group [17], which consists of the *Tyya* (metabasalts, black shales, and carbonates 1200 m thick), *Olokit* (shales, sandstones, and gravelstones), *Ondoko* (dolomites, quartz sandstones, and siltstones), and Avkit (marbles, garnet–mica schists, and quartzites up to 2500 m thick) formations. The latter two formations are probable analogues metamorphosed to different grades. Dolomites in the Olokit Formation host the Ondoko and Rybach'e occurrences of Pb–Zn ore mineralization. Amphibole–mica schists of the Avkit Formation host the Kholodninskoe Cu–Zn sulfide deposit. The stratigraphic section of the Synnyr rift begins with terrigenous–carbonate sediments of the *Ityka* (up to 950 m thick) and *Asektamur* (1700 m) formations. They are overlain by volcanic rocks of the Inyaptuk and Synnyr formations, which compose the Inyaptuk Mountains northeast of the Dovyren pluton. The age of the volcanics is 700 ± 20 Ma [35]. The Inyaptuk Formation consists of picrite-basalt pillow lavas, basalts, and basaltic andesites, along with subvolcanic trachydacite and rhyolite bodies, which are exposed in the upper reaches of the Tyya River (Morenyi Streasm). The trachydacites occasionally contain xenoliths of crystalline rocks from the Precambrian basement of the Siberian Platform. This suggests that crustal material may have participated in the generation (hybridism) of the acid volcanics in the Synnyr rift [26, 31]. Andesites and basaltic andesites of the Synnyr Formation compose the watershed part of the Synnyr Range and Mount Inyaptuk.

Information on the age and genetic relations between volcanic rocks in the Synnyr rift and the Dovyren intrusion is fragmentary. The conclusion about their genetic links was first drawn from the comparison of petrochemical materials [17]. Later it was demonstrated that some geochemical characteristics of the chilled gabbronorites and granophyre diabases in the roof of the Dovyren Massif correspond to those of basalts in the Synnyr Formation [20, 21]. This viewpoint found support in the REE patterns (Fig. 2) and isotopic ages of intrusive and volcanic rocks in the Synnyr structure, which were dated at 740 ± 55 (Rb–Sr) to 673 ± 22 (Sm–Nd) Ma [30, 33].

INNER STRUCTURE OF THE DOVYREN PLUTON

This massif is now studied more thoroughly than other intrusive bodies of the Dovyren Complex (Fig. 3). The pluton composes mounts Yoko and Dovyren, which are separated by the valley of the Ondoko River, and is, in map view, a lens-shaped body approximately ~26 × 3 km. Geophysical evidence indicates that the body can be traced to a depth of 4–5 km, i.e., the volume of the rocks composing this massifs is close to 350 km^3. The massif is subconformable with its host rocks along its strike and dip, which is nearly vertical due to postintrusive folding (Fig. 3). In spite of its Late Precambrian age, the massif is not metamorphosed. Its detailed mapping has revealed that the contour of its bottom intersects the host stratified sequence at an acute angle. This is clearly seen at the northwestern contact, where rocks of the massif cut across a carbonate bed close to the bottom of the massif, and the position of this bed before the emplacement of the intrusion is traced by xenoliths of magnesian skarns within the massif [16, 36].

The structure of the pluton varies along its strike: its central part (Mount Dovyren) includes a thick zone of ultramafic rocks, and its southwestern margin (Mount Yoko) is dominated by mafic rocks. The modal (phase) layering of the massif was thoroughly examined in its central ultramafite–mafite part, in which the bottom of the vertical section is made up of rocks of the lower contact zone (including a unit of plagioclase lherzolite) and four zones corresponding to a successive change in cumulus minerals in the Layered Series:

$$\text{Dunite } (Ol^1 + Chr) \longrightarrow \text{troctolite } (Ol + Pl + Chr)$$
$$\longrightarrow Ol \text{ gabbro } (Pl + Ol + Cpx)$$
$$\longrightarrow \text{Gabbronorite } (Pl + Ol + Cpx \pm Opx).$$

This is a generalized succession, whereas real vertical sections of the Layered Series show the intercalation and rhythmic changes in of various rock types, often with returns to more "primitive" associations [25]. A principally important unit is the lower contact [37] or reversal [38] zone, which is recognized between the main Layered Series and the rocks composing the lower inner contact zone.

Genetic importance of the Lower Contact Zone (LCZ). For the sake of further description, this term should be specified, because it is used in the petrological literature and allows for ambiguous interpretations

[1] Here and below, the following conventional mineral symbols are used: Ol—olivine, *Pl*—plagioclase, *Cpx*—clinopyroxene, *Opx*—ortho-pyroxene, *Chr*—chromite, *Phg*—phlogopite, *Sulf*—sulfide.

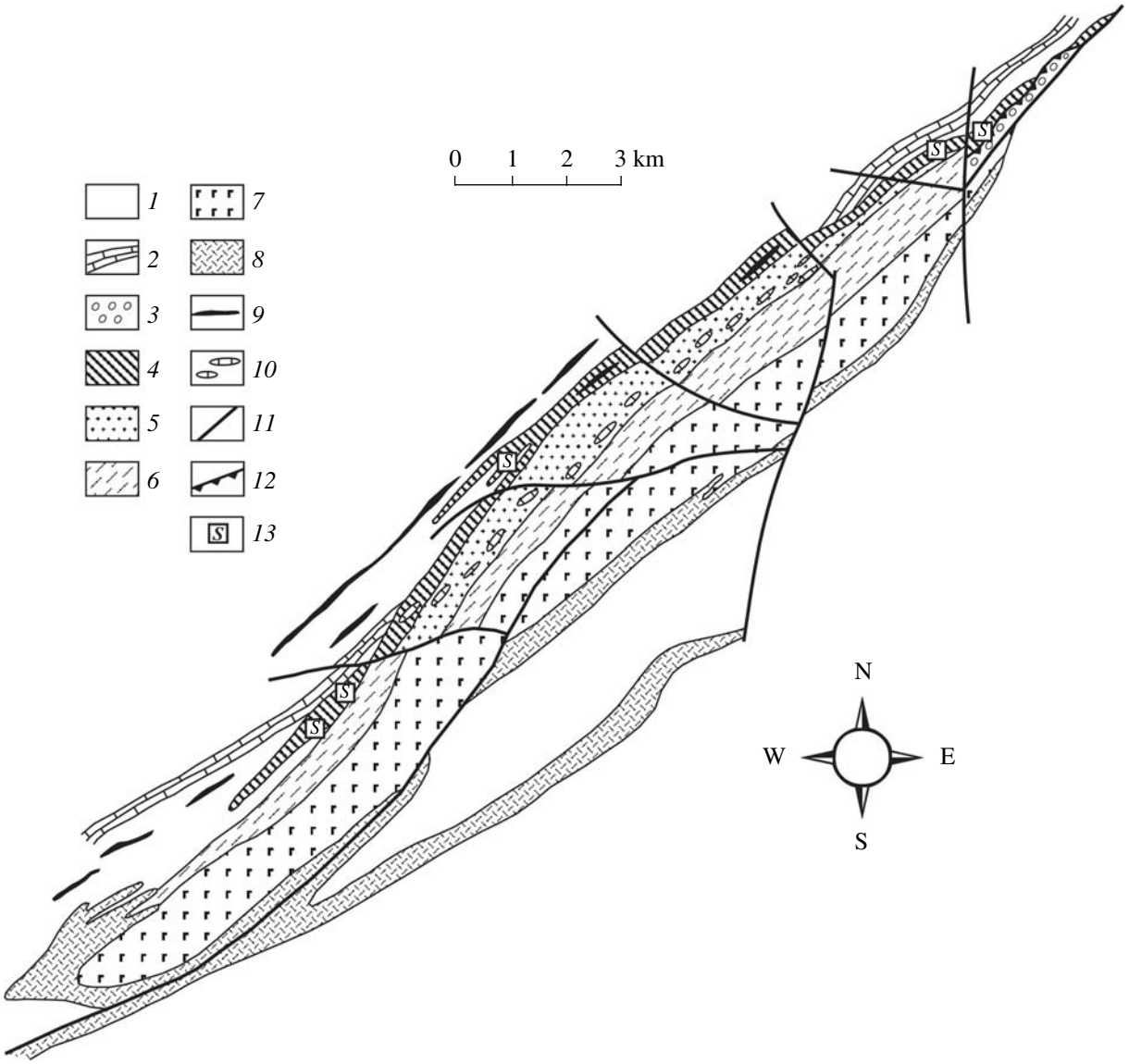

Fig. 3. Schematic geological map of the Yoko–Dovyren Massif.

(*1*, *2*) Host Late Proterozoic rocks: (*1*) terrigenous, (*2*) carbonate; (*3*) Vendian conglomerates; (*4–9*) Dovyren layered pluton: (*4*) bottom unit of plagioclase peridotites, (*5*) dunite zone A, (*6*) alternating melanotroctolite and plagioclase dunite, zone B, (*7*) olivine gabbro and gabbronorite, zones C and D, (*8*) olivine-free gabbronorite, zone E, (*9*) comagmatic (?) sills and dikes of the same composition; (*10*) xenoliths of apocarbonate magnesian skarns in dunite; (*11*) faults; (*12*) unconformities; (*13*) ore mineralization.

and is often applied to any rocks composing the lower exposed part of layered massifs. Our understanding of the LCZ is consistent with the criteria formulated in [39, 40], which were based on the comparison of numerical simulation results of the chamber differentiation of basaltic magmas with the structure of naturally occurring differentiated sills [37] and layered mafite–ultramafite intrusions as, for example, in [29]. These criteria include the spatial arrangement, petrochemical features, geochemical characteristics, and mineralogy of the rocks. All of them are consistent within the scope of the convection–accumulation model for the differentiation of intrusive magmas [37].

The name of the zone implies that the vertical section of the LCZ begins with chilled rocks of the lower inner contact of the intrusion. The absence of such rocks from exposures does not mean the absence of a lower contact zone itself but suggests that the exposed vertical section of the LCZ is reduced: a possible analogous example is provided by reconstructions for the Skaergaard intrusion [41]. Petrochemical criteria for the LCZ include the presence of a "reversal" differentiation trend expressed in coupled variations in the contents of major oxides that are seemingly at variance with the expected magma differentiation trends. These variations in most mafite–ultramafite intrusions are

pronounced as a systematic (from bottom to top in vertical sections of the bodies) enrichment of the rocks in MgO and FeO and their complementary depletion in SiO_2, TiO_2, Al_2O_3, CaO, and alkalis as, for example, in [42]. These coupled variations are associated with systematic changes in the contents of trace elements: the upward enrichment of the rocks in Ni, Co, and Cr and depletion in incompatible elements. The upper boundary of the lower contact zone is usually adjacent to a zone with the maximum MgO and Ni concentrations in the vertical section, which is referred to as crossover in [38]. The numerical simulation of chamber differentiation indicates that the diversity of the aforementioned characteristics is inevitably generated in modeled bodies if a crystalline phase settles at the solidification surface, which progressively moves upward [37]. The maximum MgO, FeO, and Ni concentrations coincide with the maximum content of cumulus olivine in the vertical section. The higher the rate of olivine settling and the slower the solidification rate, the earlier a high density of the cumulus is reached and the lower the thickness of LCZ. Hence, the distribution of compatible and incompatible elements in the low contact zones serves as a "chronometer" for the cooling rate. During the rapid cooling of relatively thin bodies, these distributions are characterized by insignificant variations, and the LCZ expands because the lower boundary shifts upward and reaches levels corresponding to 30–40% of the total thickness of the intrusion (see simulation results for the Kuz'movskii dolerite sill [37]).

In large layered massifs, variations in the chemical composition of contact rocks are contrasting and usually correlate with a change in the cumulus associations and variations in mineral chemistries. Less magnesian (supposedly "lower temperature") gabbroids and gabbronorites are spatially constrained to the contact, and they give way to more magnesian ("high-temperature") assemblages inward, up to the appearance of troctolite (*Ol* + *Pl*) and dunite (*Ol* + *Chr*). The term *high-temperature* is used here in quotation marks because the changes in the mineralogical composition of rocks and mineral chemistries in them, within the LCZ, display the final result of the continuing postcumulus crystallization and reequilibration of the original cumulus phases. This takes place at a systematic decrease in the fraction of melt captured in the intercumulus, and because of this the concentrations of incompatible components in the LCZ decrease up the vertical section (see review [22]).Thus, mineral chemistries provide not so much a record of the primary temperature as information on the porosity of the initial cumulates, the degree of their reequilibration, and the temperature of the "last volumetric" equilibrium in the closed system of crystals and residual melt [43–45]. [2] Small bodies, such as differentiated traps, display clearly pronounced petrochemical and chemical features of the LCZ, but postcumulus transformations during the rapid cooling of rocks do not modify their primary assemblages and induce less significantly the reequilibration of original minerals.

The aforementioned criteria for the recognition of lower contact zones as a typomorphic feature of crystal settling at the lower solidification front practically coincide with the characteristics of lower marginal reversals according to [38]. Although this author tried to explain their genesis and inner structure by certain physical mechanisms (whose physical action in this situation is problematic), we consider that it is possible to use the proposed term of *lower reversal* synonymously with LCZ in the context of a convection–accumulation model of differentiation. Figure 4a shows three variants of the inner structure of such reversals in naturally occurring bodies. As can be seen, these are a pervasively present constituent of so-called S-shaped profiles in the distribution of major and trace elements in the vertical sections of intrusions [46–48]. One such classic profile is presented in the right-hand diagram in Fig. 4a and demonstrates a situation when the chilled zone corresponds or is similar to the weight average of the intrusive body (parental magma). This scenario for the LCZ structure commonly occurs in relatively thin sills and intrusions whose parental magmas contain relatively little intratelluric phenocrysts [22, 37].

The central and left-hand diagrams in Fig. 4a show variants when the chilled contact zone of the intrusion consists of a less magnesian (relative to the weighted mean composition) rock, such as gabbro or gabbronorite. This situation suggests that the parental magma contained much intratelluric material and the latter was separated during magma emplacement. At olivine domination among the crystalline phases suspended in the magma (melt + olivine), a natural result of this separation is the development of rocks enriched and depleted in the initial melt. In this situation, the "low-temperature" contact gabbroids are close in composition to the liquid constituent of the parental magma, although they do not correspond to the bulk composition of the magma, deviating from the weighted mean composition of the intrusive body. This scenario is likely reflected in the structure of the LCZ of the Dovyren pluton (Fig. 4b).

The generalized vertical section through the central part of the massifs (approximately 3 km thick) clearly shows different variations in the MgO and TiO_2 concentrations in the lower inner-contact zone. The immediate contact with the host rocks consists of picritobasalts or ophitic gabbro with approximately 10 wt % MgO and 1 wt % TiO_2. Within a few meters upward from the contact, these rocks give way to olivine gabbronorites and plagioclase lherzolites with a monotonously increasing content of cumulus olivine at decreasing TiO_2 and CaO concentrations. Up the vertical section, these rocks

[2] The initial temperature at the time of settling and the origin of a crystalline precipitate can be calculated by the method of geochemical thermometry with the use of numerical models for the crystallization of basaltic magmas [12].

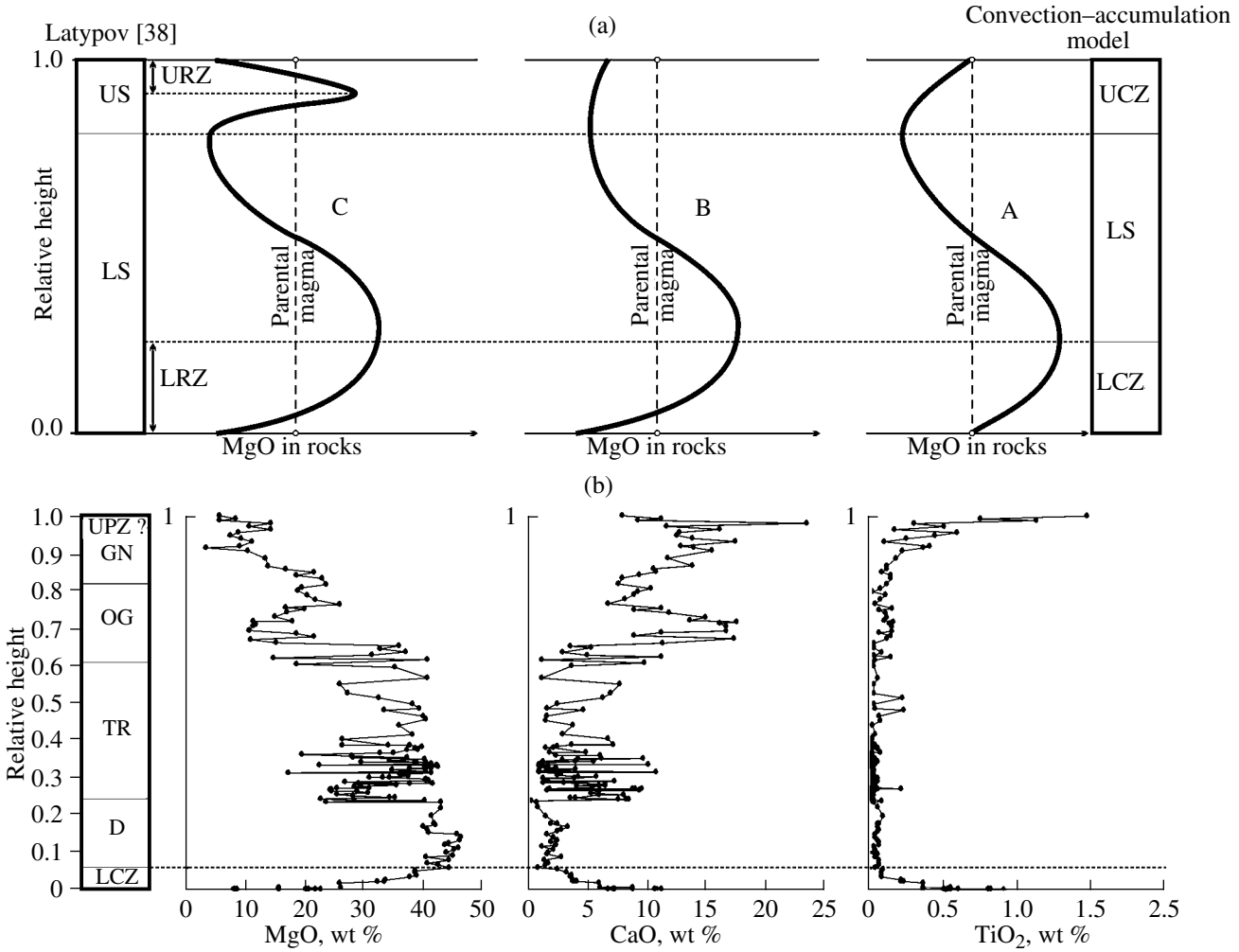

Fig. 4. (a) Possible distribution patterns of MgO in the vertical sections of differentiated sills and mafite–ultramafite intrusions and (b) the compositional variations of rocks of the Yoko–Dovyren layered massif.

(a) Reconstructions by Latypov [38]: A—the composition of the chilled rocks corresponds to the weighted mean composition of the intrusion; B and C—the composition of the chilled rocks does not correspond to the weighted mean composition of the intrusion; *US* is the upper sequence (URZ is the upper reversal zone), LS is the lower sequence (LRZ is the lower reversal zone); (b) distribution of MgO, CaO, and TiO_2 in the vertical section of the Yoko–Dovyren Massif (according to [25, 29]); UCZ and LCZ are the upper and lower contact zones, respectively, LS is the layered series, *D* is dunite, TR is troctolite, OG is olivine gabbro, GN is gabbronorite.

grade into plagiodunite with a low content of intercumulus plagioclase. The upper boundary of the LCZ in the vertical section of the Dovyren pluton was drawn by Yaroshevskii et al. [25] according to the occurrence of the densest olivine–chromite cumulates (dunites), which corresponds to no less than 40 wt % MgO in the rock and roughly coincides with the first minimum in the CaO concentration (Fig. 4b). The Ti concentration in these rocks compared to the chilled inner-contact rocks decreases by approximately a factor of ten. Our observations confirm that this structure of the inner-contact zone is repeated near the closure in the northeastern termination of the massif, although the relative thickness of the zone of plagioclase lherzolite is much lower. This suggests an elevated cooling rate and, possibly, also significant contamination with the host rocks in the marginal parts of the intrusion.

The problem of the geological setting of the plagioperidotites. Plagioclase lherzolite is readily distinguished during the geological mapping of the massif due to the occurrence of large orthopyroxene oikocrysts on the weathered surface of the rocks. This makes these rocks different from chemically similar plagiodunites. It is also easy to see, in field, that the plagioperidotites are rich in hydrosilicates (biotite and/or phlogopite) and are richer in sulfides, up to the development of sideronite textures. Mapping results indicate that the thickness of the plagioclase lherzolite "layer" in the bottom of the vertical section is estimated at 160–270 m (~200 m on average [21]), which is close to the evaluation of the LCZ thick-

ness of approximately 150 m according to [29]. The mineralogy of the plagioclase lherzolites corresponds to an association of three major cumulus phases (*Ol* + *Pl* + *Cpx*), with orthopyroxene, biotite, and, sometimes, pargasitic amphibole in the interstitial space.

The contrasting differences of the mineral composition of the plagioperidotites from that of rocks of the Layered Series (Fig. 5) and the nearly tabular morphology of the body along its strike (Fig. 3) suggest that the plagioclase lherzolites of the bottom zone of the massif can be regarded as produced by a separate portion of ultramafic weakly differentiated magma [49]. This viewpoint finds indirect support in geological evidence, indicating that plagioperidotite sills occur among terrigenous rocks underlying the Dovyren pluton and small intrusive bodies in the southeastern flank of the Synnyr rift. This interpretation implies that the variations in the proportions of cumulus minerals of the plagioperidotites in the bottom part of the massif and transitions to olivine gabbro and gabbronorite (and to picrobasalt and picrodolerite in chilled zones) characterize not the lower contact zone of the massif but the inner contacts of separate magma intrusions of plagioperidotite composition. It was also suggested [49] that plagioperidotites and the rocks of the main series of the Yoko–Dovyren massifs could result from (1) successive, with an insignificant lag, emplacement of two portions of compositionally similar peridotite magma; (2) changes in the inner-contact part of the Dovyren pluton due to the interaction of the bottom rocks with the melt "buried" in the intercumulus; and (3) selective assimilation of water and alkalis from the underlying sediments. Water assimilation in inner-contact zones explains the development of serpentinization predominantly near the bottom of the intrusion.

This viewpoint is not, however, shared by all authors of this publication, so much more that the mechanism of metasomatic rock alteration is equally applicable to both individual intrusions and inner-contact rocks of the massif. Nevertheless, we consider it necessary to mention this as an alternative mechanism for LCZ genesis. This problem will hopefully be resolved based on the detailed examination of the distribution of major and trace elements in continuous vertical sections of the Dovyren pluton. As will be demonstrated below, the nature of the plagioclase lherzolites is of principal importance for the evaluation of the temperature and composition of the magmatic melt during the emplacement of the Dovyren magma.

The inner structure of the Layered Series. Figure 5 exhibits the schematized inner structure of the Yoko–Dovyren intrusion (the schematic section was prepared at the Geological Institute of the Siberian Branch of the Russian Academy of Sciences based on materials obtained by studying sections in the central part of the massif). The proportions of the major zones of the layered series (A, B, C, and D) in this section are not principally different from those in the scheme in [24, 25]. The only principal deviations pertain to the geological position of the roof rocks. Yaroshevskii et al. consider the predominant olivine-free (granophyric) gabbronorite and quartz gabbro of this zone to be the final member of the layered series (zone E). An alternative interpretation implies that the layered series of the Dovyren intrusion ends with olivine gabbro and gabbronorite, and the overlying rocks of the roof zone were formed by an autonomous granophyre diabase intrusion [20]. Similar to the bottom rocks, this problem can be solved based on further investigations aimed at the detection of systematic spatial variations (or their absence) in the composition of the rocks and minerals composing the roof part of the massif. It can now be admitted that the petrochemical data and variations in rock compositions in the vertical sections presented in [25, 29] do not contradict the idea that the granophyric gabbronorites and quartz gabbro are residual systems, which were formed by the chamber differentiation of the Dovyren magma. This does not rule out the possibility that autointrusions of such residual magmas could take place late during the solidification of the Dovyren massif and occur in the massif itself and the overlying rocks. Below we present a description of the Layered Series of the intrusion.

Zone A: the section of dunite is ≤980 m thick and includes olivine meso- and adcumulates. Olivine (80–97 vol %) occurs as subhedral crystals, with the interstitial space filled with Cr-spinel and plagioclase. The content of plagioclase in the dunites increases closer to the plagioperidotites. The mg# of olivine decreases toward the contact: the average *Fo* concentration in olivine is 87.4 mol % in the dunite, 86.7 mol % in the plagiodunite, and 85.3 mol % in the plagioclase lherzolite [21, 22]. This trend is inconsistent with the "normal" evolution of compositions during crystallization and may be an indication of the transition to the lower contact zone (see the discussion on the inner structure of the marginal group in the Burakovskya intrusion in [42]). The central part of the dunite section contains olivine with 89–90% *Fo*. The maximum mg# of the mineral ($Fo_{92–98}$) was found at the upper levels, near contacts with xenoliths of magnesian skarns. Such rocks with elevated MgO and CaO concentrations (up to 0.9 wt %) in their olivine often have an adcumulate structure and texture and are contaminated dunites [23]. Domains with xenoliths of magnesian skarns (that replaced carbonates) are characterized by high-Ca clinopyroxene, which takes the place of plagioclase in the adcumulus. The appearance of intercumulus clinopyroxene in these rocks is explained by the CaO assimilation from carbonates. The content of diopside often reaches 50 vol %, and the dunites grade into wehrlites with a poikilitic texture. Clinopyroxene sometimes forms patches and irregularly shaped veins in dunites, and the latter acquire a taxitic structure. The Al_2O_3 concentration in the clinopyroxene reaches 6.6 wt % [50].

Zone B: consists of troctolite (~700 m), which replaces dunite (Fig. 5) and consists of alternating melanotroctolite (30–50 vol % plagioclase) and plagioclase

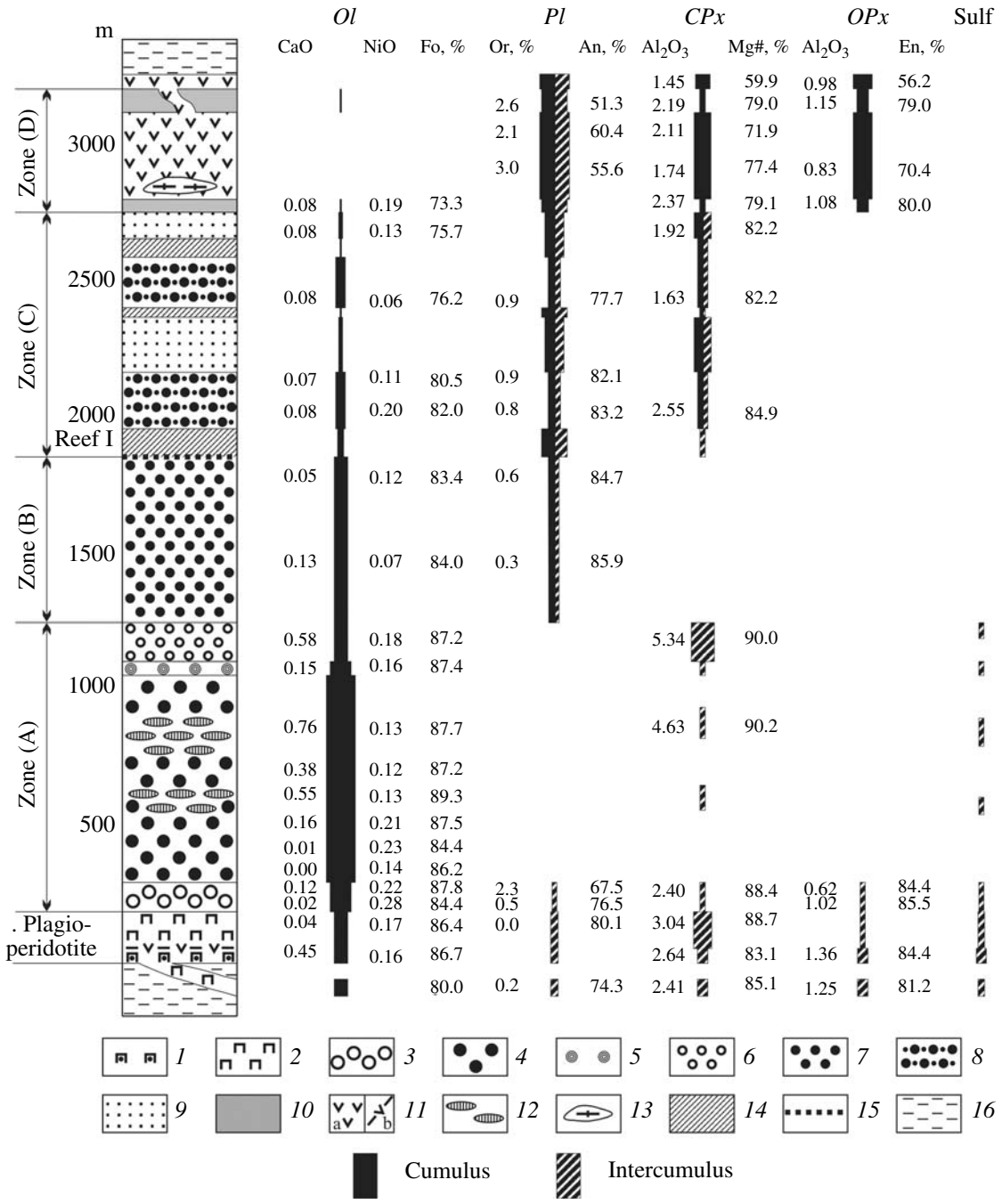

Fig. 5. Schematic vertical section of the Yoko–Dovyren Massif based on data on mafite–ultramafite sections examined in the central (thicker) part of the intrusion.

(*1*, *2*) LCZ: (*1*) chilled picrobasalts and ophitic gabbro, (*2*) phlogopite- and plagioclase-bearing lherzolites; (*3–6*) zone A: (*3*) plagiodunite, (*4*) monomineralic dunite, (*5*) wehrlite, (*6*) diopside-bearing dunite; (*7*) zone B: alternating troctolite and plagiodunite; (*8*, *9*) zone C: (*8*) olivine gabbro, (*9*) leucocratic gabbronorite; (*10*, *11*) zone D: (*10*) olivine norite, (*11*) pigeonite granophyric gabbronorite from (a) the upper contact and (b) the dike in LCZ; (*12*) xenoliths of magnesian skarns; (*13*) xenoliths of granophyres in zone D; (*14*, *15*) anorthosite and gabbro-pegmatite layers with low-sulfide PGE mineralization; (*16*) host rocks.

dunite (5–20 vol % plagioclase) These rocks were formed when the residual melt became saturated with olivine and plagioclase as cumulus phases. The rocks have an allotriomorphic-granular texture, which is characterized by equally euhedral rock-forming minerals. The content of interstitial pyroxene rarely exceeds 2–3 vol %, but the upper part of the zone includes units enriched in augite (poikilitic wehrlites) and lenses of olivine gabbro compositionally similar to the rocks of the next zone.

Zone C: includes predominantly olivine gabbro and has a thickness of ~350–400 m. It differs from the underlying rocks in having much less olivine and in containing augite. The predominant cumulus mineral is plagioclase. Its lath-shaped crystals are included in olivine and clinopyroxene grains. The texture of the rocks is gabbroic and gabbro-ophitic. The olivine gabbro in the lower part of intrusion include numerous gabbro-pegmatite veins which are characterized by a taxitic structure including anorthosite segregations with disseminated sulfides containing PGE and Au mineralization.

Zone D: is dominated by gabbronorite (≥600 m). The bottom of this unit is marked by the appearance of individualized layers of olivine norite and olivine gabbronorite. These rocks are in complicated intercalation relations. The olivine gabbronorite is characterized by the occurrence of large (3–5 cm) orthopyroxene oikocrysts. The texture of the rocks of gabbroic, and the cumulus minerals are large olivine grains, short-columnar plagioclase crystals, prismatic clinopyroxene grains, and orthopyroxene.

Zone E [24]: comprises roof gabbro and granophyric gabbronorite (250–350 m) devoid of olivine. These rocks contain no Cr-*Spl*, which is a typical mineral of all underlying rocks, and the accessory minerals are ilmenite, titanomagnetite, and apatite. The texture of the rocks is dominated by tabular grains of zonal labradorite-andesine, hypersthene, and augite, and the interstices are filled with amphibole, biotite, and granophyre. According to the chemical and modal composition of the rocks, this zone is analogous to sills and dikes cutting across the bottom plagioperidotite. It is also known that the bottom and roof are granophyre gabbronorite and converge in the southwestern tapering of the massif (Fig. 3). This argument was the reason for excluding the olivine-free rocks from the section of the Layered Series of the Yoko–Dovyren massifs [20].

PROBLEMS OF THE PETROLOGY OF THE DOVYREN MASSIF

The petrologic aspects of the genesis of the Dovyren intrusion can be grouped according to the following problems (1) the emplacement of the Dovyren magma and the genesis of the lower contact zone; (2) the genesis of the inner structure (layering) of the massif, including the problem of the nature of the high-Mg dunites; and (3) the scale and role of the assimilation of host rocks.

Crystallization conditions of the parental magma. According to geological data, the Dovyren intrusion was emplaced at a depth of 1.5 km [18], which corresponds to a total pressure $P \sim 0.5$ kbar. This is consistent with pressure estimates based on the composition of apocarbonate magnesian skarns [36, 51]. It is more problematic to evaluate the oxygen fugacity. Based on known data on the degree of oxidation of natural magmas and with regard for magnetite absence among the cumulus minerals in the Layered Series of the massif, Ariskin et al. [22] concluded that the conditions were relatively reduced, close to the wustite–magnetite (WM) buffer. These estimates are close to that in [23], where it was demonstrated that olivine–chromite equilibria in the uncontaminated dunite zone of the Dovyren intrusion correspond to $\log f_{O_2}$ values roughly one unit below the QFM buffer. Judging from the absence of hydroxyl-bearing minerals from the layered series of the massif and the occurrence of antiperthitic potassic feldspar ingrowths in plagioclase from the gabbroids, the Dovyren magma was undersaturated in H_2O [21]. Then, with regard to the above-mentioned estimate, the water content in the initial magmatic melt was no higher than ~0.5 wt %.

Composition of the Dovyren magma. The bulk composition of the parental magma (a mixture of crystals and melt during the emplacement of the magma) in a closed magmatic chamber should correspond to the weighted mean composition of the massif. The solution of this problem involves the evaluation of the average compositions and relative volumes of rocks in various vertical sections, including those through the marginal zones of the Dovyren pluton. Although this problem has been explored for many years, it has still not been solved. Fairly detailed information was obtained on the diversity [20, 21, 24] and average petrochemical types of rocks of the Layered Series [25], but their relative volumes remain uncertain. Current evaluations of the composition of the Yoko-Dovyren intrusion are based on data obtained on a number of vertical sections through the thickest central part of the massif, where the thickness of dunite reaches 700–980 m. The closure parts of the massif in its northeastern and southwestern terminations, which contain practically no compacted adcumulus dunite, are inadequately, poorly studied. As was mentioned above, the variations in the relative thickness of the lower contact zone along its strike are also unclear. A separate problem is the absence of an upper contact zone, which usually consists of the Upper Marginal Group in layered massifs, with rock compositions of this group mirroring the variations in the mineralogy and chemistry of the rocks of the Layered Series [52]. Table 1 reports two estimates for the supposed composition ("parental magma") of the Dovyren pluton that are based on detailed data on vertical sections [28, 29]. The fourth column shows the weighted mean composition of the generalized vertical section through the central part of the massif (approximately 3 km thick [29]), and the sixth column lists the "integral" composition from [28][3]

[3] According to E.V. Koptev-Dvornikov (personal communication), this vertical section was composed of a contact zone, which was sampled in the area of the Tsentral'nyi Creek, and main vertical section no. 4, which was examined approximately 7 km northeast of it, in the area of the Belyi Creek, on the northwestern slope of Mount Dovyren, and, with an upstrike shift, in the upper part of the section on the opposite slope.

Table 1. Chemical and phase characteristics of the "parental magmas" of the Yoko–Dovyren layered intrusion: computer simulations by the COMAGMAT software package

Oxide	[22]			[29]		[28]	
	Average composition of the initial melt	Calculation for the average composition of the chilled rocks (P = 0.5 kbar, T = 1185°C)		Calculation for the average composition of the massif (P = 1 kbar, T = 1340°C)		Calculation of the "integral" composition of the massif (P = 1 kbar, T = 1402°C)	
		"Parental magma"	Melt	"Parental magma"	Melt	"Parental magma"	Melt
SiO_2	54.13	47.71	55.00	43.92	45.95	46.12	47.44
TiO_2	0.78	0.36	0.74	0.11	0.18	0.31	0.39
Al_2O_3	15.24	9.11	15.52	9.72	15.93	9.88	12.46
FeO	8.19	10.37	7.58	10.53	10.88	10.50	10.98
MnO	0.15	0.15	0.14	0.17	–	–	–
MgO	7.51	24.75	7.33	27.88	14.49	24.07	17.24
CaO	11.33	6.03	10.80	6.99	11.46	7.81	9.85
Na_2O	1.65	0.94	1.72	0.59	0.97	0.71	0.90
K_2O	0.88	0.54	1.08	0.07	0.11	0.53	0.67
P_2O_5	0.14	0.04	0.08	0.02	–	0.06	0.08
Phase composition of the parental magma, wt %							
Melt	–	48.9	–	~60	–	76	–
Ol	$Fo_{84.6 \pm 1.0}$	46.5	$Fo_{85.3}$	~40	$Fo_{89.7}$	24	$Fo_{91.2}$
Pl	$An_{80.5 \pm 4.5}$	4.6	$An_{79.8}$	–		–	
F	–	51.1		~40		24	

Note: The compositions are normalized to 100%. The initial melt in the first column corresponds to an average of ten compositions of model liquids at 1185°C [22]; the composition of chilled rocks ("parental magma") is according to [53]; the "integral" composition of the massif was calculated by the method [28], F is the content of crystals in the system (crystallinity of the parental magma).

Another potential source of information on the composition of the Dovyren magma is plagioperidotite sills up to 200 m thick, which were mapped below the bottom of the massif. These sills are concentrated in the outer-contact terrigenous rocks of approximately 300 m in total thickness (Fig. 3). The geological relations imply that these autonomous bodies belong to the same magma plumbing system as the Dovyren pluton itself and may provide material corresponding or close to that of the parental magma that produced the massif [20]. The sills are heterogeneous: field observations indicate that the sills are differentiated into gabbroids (~10% MgO) and ultramafites (~30% MgO) [21], and that the latter are plagioclase lherzolites analogous to plagioperidotites in the bottom of the massif. Assuming that these components are contained in the proportion 1 : 3, we arrive at a parental magma containing approximately 24 wt % MgO. A more precise evaluation requires more detailed data on the vertical sections through these bodies. Another possibility for evaluating the composition of the Dovyren magma is studying chilled rocks that show evidence of the minimum separation of their suspended phases and thus corresponding to the parental melt–crystal mixture. Such rocks were found in the bottom of the massif and were described in the literature as chilled ophitic gabbro or picrodolerites [18, 21, 53]. All of these rocks are characterized by high MgO concentrations (19–25 wt %) and abundant olivine phenocrysts. As an example, the second column of Table 1 presents the average composition of the chilled rocks (according to [53]), which is characterized by the maximum MgO concentration and the maximum content of modal olivine (42 vol % on average). This composition was used in our thermometric simulations of the initial magmatic melts of the Dovyren intrusion [22].

Composition and temperature of the magmatic melt. The application of the olivine–melt thermometers [12] in evaluating the composition of the Yoko–Dovyren parental magma (Table 1) indicates that, if this magma was hot, it should have contained olivine of the composition ~Fo_{94}. This is notably different from data on the olivine composition from the bottom of the vertical section (Fig. 5) and suggests that the magma emplaced into the chamber was a suspension of solid phases and melt. This conclusion finds support in data on the chilled contact rocks of the massif, which contain up to 40–50% modal olivine.

The first attempt to separate the problems of evaluating the composition of the Dovyren magma and the

initial magmatic melt was undertaken in [54]. The authors of this publication used the composition of an inner-contact chilled rock from a plagioperidotite sill comagmatic with the massif (24.4% MgO) in mass-balance calculations based on the subtraction of 30% olivine phenocrysts. The resultant predicted MgO content in the magmatic liquid was 15.7 wt %. This picrobasalt composition was not controlled by calculations with the use of K_d(Fe-Mg) olivine–melt to elucidate whether the modeled olivine composition is realistic. A more systematic approach was applied in [33], whose authors noted that olivine in the dunites contains approximately 87 mol % forsterite (Fig. 5), and this composition coincides with the composition of an olivine inclusion in chromite from the lower part of the dunite unit [55]. This composition was assumed as the average equilibrium composition of olivine phenocrysts, and this made it possible to estimate the mg# of the initial melt with the use of K_d(Fe–Mg) = 0.30. The value of mg# = 0.675 was then utilized in the graphic reconstructions of the composition of the dunite, plagioperidotite, and inner-contact gabbronorite. The comparison of the olivine control lines in an MgO–FeO plot gave an evaluation of the concentrations of these oxides in the melt, and these values were consistent with the assumed olivine composition (Fo_{87}) and established petrochemical trend: 7.75 wt % MgO and 6.65 wt % FeO. These concentrations corresponded to a gabbronorite, but not a picrobasalt, melt.

We carried out COMAGMAT simulations for the equilibrium crystallization of chilled inner-contact rocks, bottom plagioperidotites, and the weighted mean composition of the intrusion at P = 0.5 kbar at the WM buffer [22]. With regard for the accuracy of the applied plagioclase geothermometers, our results pointed to the subcotectic ($Ol \pm Pl$) nature of the Dovyren magma, whose temperature during its emplacement was 1180–1190°C, and the equilibrium olivine had the composition ~Fo_{85}. Chemical characteristics of these modeled melts are reported in the first and third columns of Table 1. Note that they practically coincide with the estimate for MgO in [33] but suggest a higher FeO concentration of approximately 10.5%. These values confirm the principal conclusion about the gabbronorite composition of the initial magmatic melt. Indirect evidence in support of this conclusion is the wide occurrence of gabbronorite dikes in the rocks surrounding the massif.

Simulations based on the convection–accumulation model. Recent results on the numerical simulation (by the intrusive version of the COMAGMAT model [12]) of the integral vertical section of the Dovyren massif were published in [29]. This work was an attempt to interpret petrochemical features of the lower contact zone and the Layered Series of the massif within the scope of the convection–accumulation model for chamber differentiation [37, 56] and was aimed at the simulation of the distribution of major elements over the vertical section, with this distribution interpreted within the framework of the model as resulting from variations in the ensemble of the cumulus phases and their proportions and in the amount of captured or intercumulus melt. The composition of any rock in the vertical section is thereby specified by a mass balance equation

$$C^i_{\text{rock}} = f_l C^i_l + \sum_{j=1}^{m} f^{\text{cum}}_j C^i_j, \quad (1)$$

where C^i_{rock}, C^i_l, and C^i_j are the concentrations of component i in the rock, intercumulus melt, and cumulus phases ($1 \le j \le m$), and f_l and f^{cum}_j are the contents of melt in crystals in the cumulus. It is assumed in this model that the composition of the intercumulus melt corresponds to the composition of the fractionated liquid in the bulk volume of the residual spontaneously stirring (convecting) system. The composition of the cumulus phases vary corresponding to the crystallization sequence of the parental magma and are in thermodynamic equilibrium with residual (intercumulus) melt at any moment of time (which corresponds to the position of the rock-forming system in the vertical section). The proportions of cumulus and intercumulus are a function of the cooling rate and the effective sedimentation of the phases and depend on certain fitting thermophysical parameters of the model [37].

The simulation of the petrochemical structure of a magmatic body by this model is an example of direct modeling, when the researcher deals with the "response" of the system to the assumed initial conditions and fitting parameters. The simulation results are compared with natural data, the predictions are corrected, and the simulations are resumed until a consistency is reached (if possible) between the observed and modeled characteristics. Thereby any bends of the petrochemical trends or a drastic change in the concentrations of major or trace elements are explained as resulting from the evolution of the phase composition of the modeled cumulate, including a fraction of the intercumulus liquid. Applying this approach to the assumed composition of the parental magma, the authors of [29] managed to fit the initial emplacement parameters and a set of thermophysical parameters that made it possible to reproduce, in much detail, the petrochemical features of the vertical section of the Dovyren pluton (Fig. 6). These data testify to a much higher temperature (1340°C) and a much more magnesian composition of the melt in equilibrium with olivine of the composition $Fo_{89–90}$ (Table 1).

Correction for the compaction of cumulates. Although Bolikhovskaya et al. [29] managed to numerically simulate the principal features of the distribution of major elements in the vertical section (Fig. 6), these researchers did not elucidate certain issues concerning the possibility of the convective stirring of significantly crystalline suspensions and the simultaneous development of a compact cumulus corresponding to dunite. The thing is that the physical driving force for the development of convection flows from the roof of an

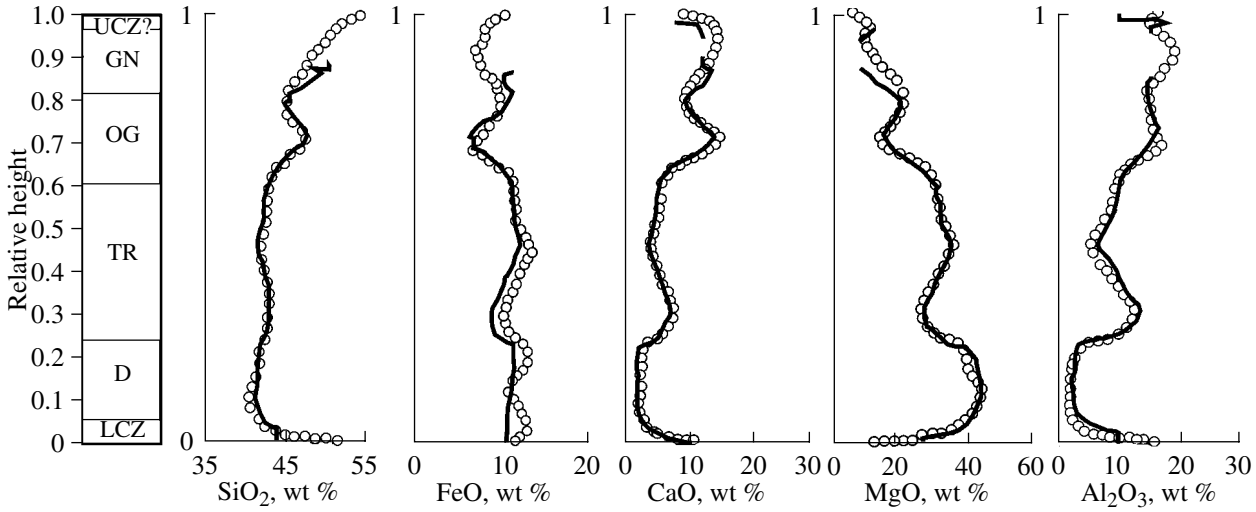

Fig. 6. Observed (circles) and simulated (lines) distribution of major elements in the generalized vertical section of the Dovyren Massif [29].

The simulations were conducted by the convection–accumulation model for the differentiation of intrusive magmas [37]. The parameters of the parental magma are listed in Table 1. The "observed" compositions are real compositions of rocks from the generalized vertical section processed by the sliding window technique.

intrusion is density inversion in the upper boundary layer and the origin of suspensions that are denser than the residual magma occupying the bulk volume of the chamber [37, 56]. The results obtained by the convection–accumulation model imply that residual melts always contain no less than 40–50% crystals (see Fig. 5 in [29]). It should be thereby assumed that even denser suspensions can be produced in the boundary layer and contain 60–70% crystals (in fact, a compact cumulus), which could sink through the residual magma and maintain "free convection" in the mush of crystals and residual melt 3 km thick. From the physical viewpoint, it is also hard to admit the possibility of the direct developments of olivine "precipitate" with 90–95% crystals, which ensures the origin of dunite with 35–40% MgO in the model (Fig. 6).

These considerations gave rise to the hypothesis that the predominant processes in the magmatic chamber of the Yoko–Dovyren Massif were (at least early in the course of solidification) the settling of intratelluric olivine, the compaction of the produced cumulus, and the migration of the pore liquid corresponding to the initial melt [22]. The bottom part of the chamber was not thereby involved in large-scale convection according to the mechanism of descending and ascending suspension flows. These ideas were further developed in the *convection–compaction model of differentiation* [28]. This author modified the intrusive block of the COMAGMAT software package [12] to develop a two-layer model, in which a regime of freely convecting magma occurs in the upper part of the chamber and heat and mass transfer related to the compaction of the cumulus and the coupled removal of the intercumulus melt should be accounted for in the lower part of the chamber. Searches for the optimum parameters of the convection–compaction model in application to the Dovyren intrusion were accomplished for a parental magma of composition close to the average composition of the chilled rocks, under the assumption of ~20% intratelluric olivine phenocrysts (Table 1). The temperature at which the magma was emplaced was evaluated at 1400°C, and the liquid constituent of the initial suspension had a komatiite composition (17–18 wt % MgO) and was in equilibrium with olivine of the composition ~Fo_{91}. These simulations led Lavrenchuk [28] to reproduce the principal tendencies in the distribution of major elements in the lower contact zone of the Layered Series of the Yoko–Dovyren Massif (Fig. 7). The modeled dunite, which contains up to 95% cumulus olivine, was interpreted as produced by the compaction of the cumulus and the continuing adcumulus growth of olivine grains.

The results of the forward and inverse simulation of the physicochemical parameters of the Dovyren magma led to constraining the possible temperatures and compositions of the magmatic melt during its emplacement. These estimates vary from high-Mg komatiite (17.2% MgO) and picritic (14.2% MgO) compositions in equilibrium with olivine $Fo_{91–89}$ at 1400–1340°C [28, 29] to moderately magnesian gabbronorite melt (~7.5% MgO) in equilibrium with Fo_{85} at ~1185°C [22]. All three groups of the researchers arrived at the conclusion that the parental magma and contained from 20 to 50% olivine phenocrysts. Such a broad scatter of the possible parameters of the Dovyren magma puts forth the problem of their more accurate determination, first and foremost, the more accurate constraining of the temperature and composition of the

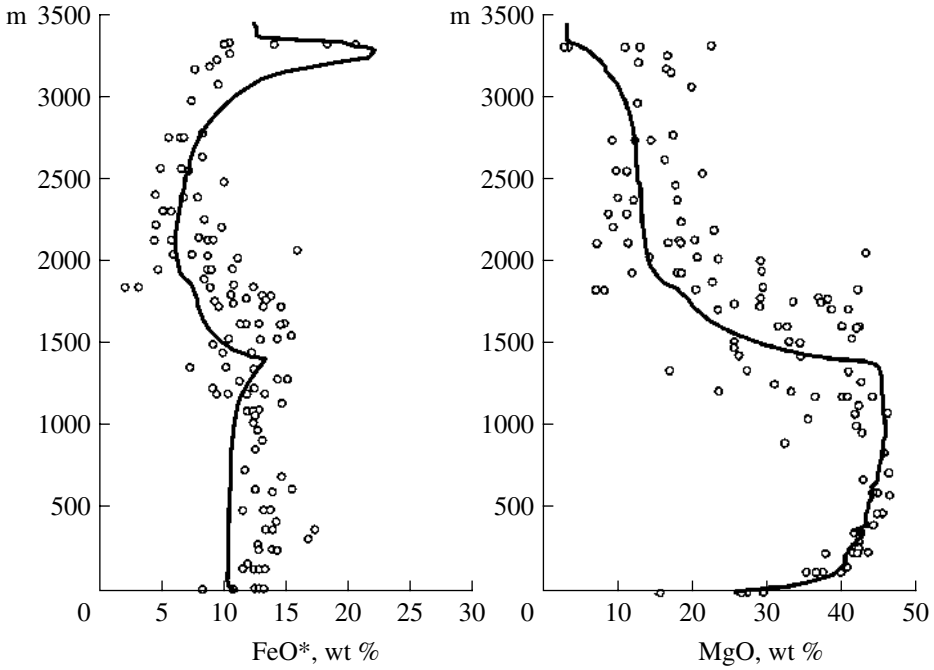

Fig. 7. Observed (circles) and simulated (lines) distribution of FeO and MgO in the vertical section of the Dovyren Massif [28]. Simulation results by the convection-compaction model for chamber differentiation. The parameters of the parental magma are listed in Table 1. The observed compositions are real compositions of rocks according to [21, 27]. FeO with asterisk denotes Fe_{tot}.

magmatic melt, i.e., parameters that controlled not only the detailed structure of the massif but also the sulfide potential of the initial system and its potential to form Cu–Ni sulfide mineralization.

Importance of the olivine control lines. Regardless of the assumed temperature and composition of the parental magma (Table 1), the genesis of the plagioperidotite and plagiodunites in the lower contact zone of the Dovyren Massif can be explained by variations in the content of cumulus olivine in the intercumulus liquid (Figs. 4, 6, 7). This makes it possible to estimate the plausibility of the simulations by applying additional criteria underlain by mass balance for systems saturated with olivine. Indeed, when the cumulus phase is only olivine of constant composition, Eq. (1) can be brought to the form

$$C^i_{\text{rock}} = f_l(C^i_l - C^i_{Ol}) + C^i_{Ol}, \quad (2)$$

where C^i_{Ol} is the concentration of component i in the intratelluric (cumulus) olivine. Then, for any pair of chemical elements, it can be written

$$C^1_{\text{rock}} = aC^2_{\text{rock}} + C^1_{Ol} - aC^2_{Ol}, \quad (3)$$

where

$$a = (C^1_l - C^1_{Ol})/(C^2_l - C^2_{Ol}) = \text{const}. \quad (4)$$

According to (3, 4), the compositions of olivine cumulates in variation diagrams should be fitted by linear trends (tie lines) connecting the compositions of the intercumulus liquid and initial olivine at the moment of time when the cumulus was formed. Such relations are known in petrology as *olivine control lines* [57]. At the hypothetical 100% compaction of a crystalline precipitate, these trends pass into the composition of the initial (intratelluric) olivine. Hence, the bulk compositions of natural plagioperidotites and plagiodunites should contain a record of the composition of their cumulus primary olivine, and this information can be recovered using olivine control lines (see, for example, [42, 58]). Note that the desired information is "recorded" in the bulk compositions of the rocks but not in olivine compositions (that can be analyzed on a microprobe), because the latter can result from postcumulus reequilibration [43–45]. When cumulus crystallizes as a closed system or is compacted with the partial segregation of the intercumulus liquid, the final olivine composition is always more ferrous than that produced during the accumulation of the crystals. The bulk composition of the mixture of crystals and melt can shift along the only tie line corresponding to the average composition of the initial olivine brought by magma into the chamber.

Figure 8 exhibits olivine control trends depending on the MgO concentration for the plagioperidotites, plagiodunites, noncontaminated dunites of the Yoko–Dovyren Massif (below 200 m in the vertical section of the intrusion), and for some rocks from the comagmatic sills [21, 50]. The diagrams also show tie lines connecting the compositions of the initial melt and olivine for three characteristics of the Dovyren magma listed in

Table 1 [22, 28, 29]. These lines are interesting because they provide unambiguous estimates for the composition of the orthocumulates and adcumulates in the LCZ that could be formed from such mixtures of olivine crystals and melt. Obviously, if the parameters of the parental magma are plausible and realistic, the tie lines should coincide with the compositional trends of the rocks making up the lower contact zone. As can be seen, the trends of the natural rocks in Al_2O_3–MgO and CaO–MgO diagrams are localized between the model tie lines, and the composition [29] has an obviously overestimated Al_2O_3 concentration. The differences between the modeled sequence are more contrasting in the SiO_2–MgO plot. For the lowest temperature mixture of gabbronorite melt and olivine Fo_{85} [22], the natural and modeled sequences are close and practically parallel. At the same time, tie lines in [28, 29] intersect the evolution trajectory of the natural compositions toward more silicic "rocks". The most principal differences are revealed by an analysis of the FeO–MgO trends (Fig. 8). The natural trend for the chilled gabbronorites to plagiodunites intercepts the stoichiometric olivine line at ~$Fo_{84–86}$. This estimate and this trend correspond to a tie line constructed based on data from [22]. Tie lines based on the results in [28, 29] "shift" the petrochemical characteristics of the modeled rocks in the compositional region depleted in FeO compared to natural rocks. This depletion is more clearly pronounced for the composition [28] (Table 1) and reaches 2–3 wt % FeO at MgO concentrations within the range of 30–40%. These relations allow us to consider the distribution of oxides in Figs. 6 and 7 from another standpoint. In both instances, the compositions of the modeled rocks include underestimated FeO concentrations. The data of Fig. 8 demonstrate that this inconsistency directly follows from the overestimated temperatures and mg# of the initial magmatic melt. Obviously, the rocks corresponding to the plagioperidotites and plagiodunites of the LCZ could not result from olivine accumulation in high-temperature melts with >10 wt % MgO.

This conclusion is not only of a genetic but also of a methodical importance. The example of the above considered natural and simulated trends highlights the hazard of the visual comparison of observed and simulated distributions of oxides during searches for the optimal parameters of the convection–accumulation [29] or convection–compaction [28] models. For a system oversaturated with respect to olivine, the results of such simulations should necessarily be checked by analyzing olivine control lines to reach (if possible) the best consistency between the simulated contact rocks and the tie lines between the initial melt and initial olivine. A good consistency of the modeled trend [22] with the natural characteristics does not mean that the Dovyren chamber was replenished with gabbronorite melt containing olivine of the exact composition Fo_{85} at 1185°C. Now we regard this estimate as the lower limit for the possible temperature of the parental magma. The analysis of data in Fig. 8 indicates that the natural trends can also be consistent with melts containing olivine $Fo_{86–87}$. The estimates for the initial olivine composition can be specified based on a more thorough sampling of the contact zone of the massif with the collection of samples of as fresh as possible plagioperidotites and plagiodunites. It is important for the analytical data on rocks to be consistent, best of all, to be obtained at the same laboratory.

The problem of high-Mg olivine in the dunites. The FeO–MgO distribution shows a clearly pronounced compositional trend of the Dovyren dunites, which is roughly parallel to the olivine stoichiometry line and intersects the olivine control line for the parental magma (Fig. 8). Olivine in the dunites displays broad compositional variations: from 82 to 90 mol % of the forsterite end member. These relations cannot be explained by the trivial schemes of crystallization differentiation. Obviously, this "dunite" trend cannot be accounted for by variations in the cumulus–intercumulus proportions alone. If the Dovyren magma contained at the time of its emplacement olivine of the composition $Fo_{85–87}$, one should surmise some mechanism for the origin of the dunites the chamber, with these rocks containing olivine of more ferrous (<85% *Fo*) and more magnesian (>87% *Fo*) compositions. In the former instance, it can be assumed that the original olivine underwent reequilibration with the trapped melt in the lower part of the Dovyren chamber, and this process was associated with the pressing out of the residual and relatively lower temperature liquid. The possibility of such olivine recrystallization in the process of postcumulus cooling of mafic–ultramafic magma is not doubted. The situation with the genesis of more magnesian olivine is more complicated: this olivine could not result from the crystallization of the parental melt and redistribution of phenocrysts. Below we consider a number of alternative possibilities within the scope of the concept of a closed magmatic chamber.

(1) It can be hypothesized that the magmatic material that filled such a large reservoir could be heterogeneous both in the composition and temperature. The simulation of the filling process of funnel-shaped chambers demonstrates that the peripheral (near contact) zones of the intrusions are produced by the crystallization of relatively low-temperature magma from the boundary layer of the magma conduit [59]. The forced flow of hotter and more primitive magma from the central part of the magma conduit was responsible for the filling of the bulk volume of the intrusive chamber.

(2) An increase in the oxygen potential in the crystallizing system in response to the assimilation of carbonates [50]. Data of Pushkarev et al. [23] indicate that the differences in the $\log f_{O_2}$ values during the origin of uncontaminated and contaminated dunites in zone A (Fig. 5) were approximately two orders of magnitude, and the uncontaminated olivine crystallized were under more reduced conditions. The assimilation of carbonates resulted in a decrease in the Fe^{2+}/Mg ratio of the melt, and this induced an increase in the mg# of the

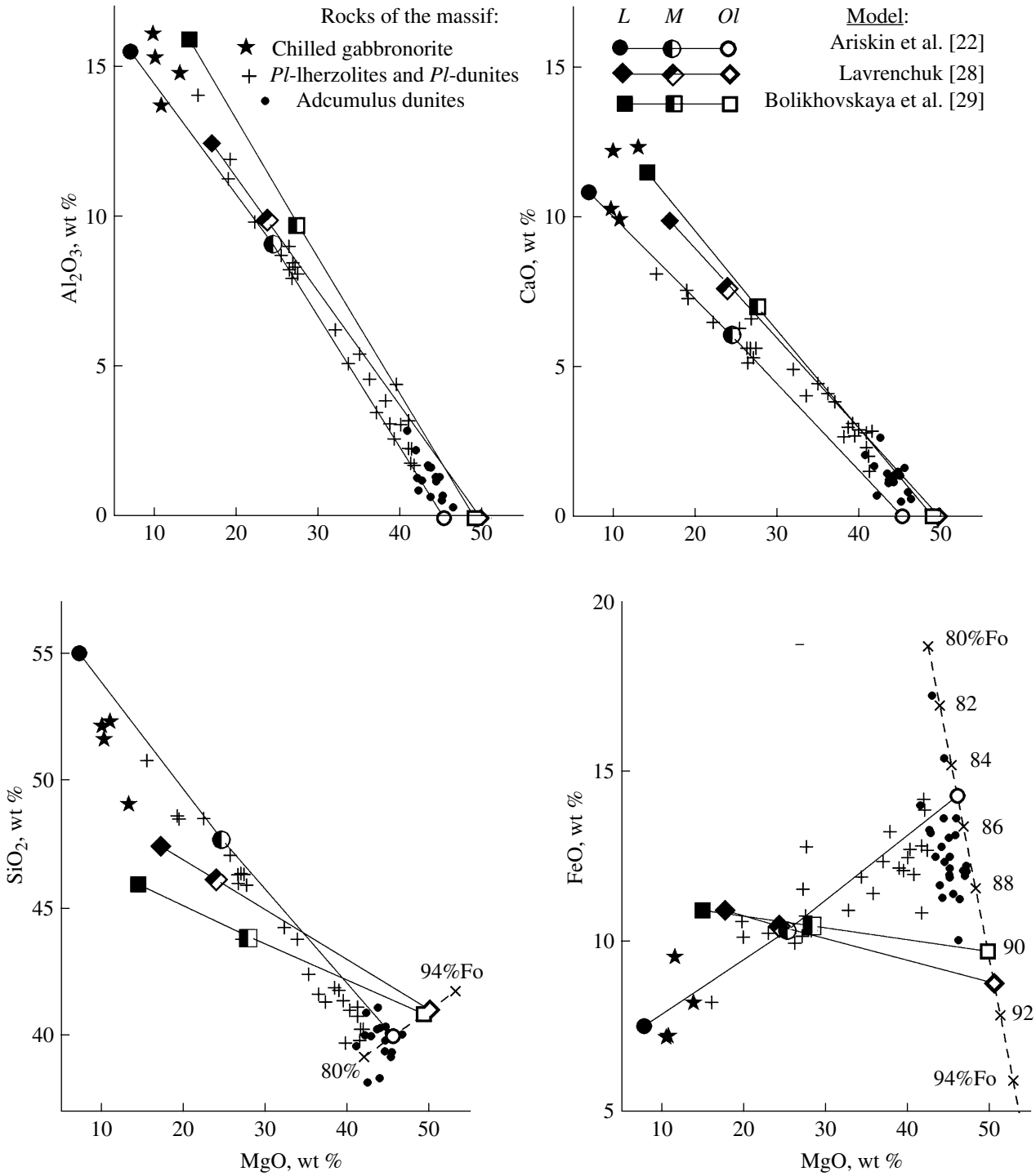

Fig. 8. Compositional trends of LCZ rocks and dunites of the Yoko–Dovyren Massif in comparison with olivine control lines based on evaluations of the temperature–compositional characteristics of the parental Dovyren magma.

Compositions of rocks from the bottom of the Yoko–Dovyren Massif (below 200 m): plagioperidotites, plagiodunites, and dunites are according to [21, 50], chilled gabbronorites are according to [21, 33]. Tie lines for compositions of the parental magma are based on data from Table 1: *L* is the initial melt, *M* is magma, *Ol* is the composition of the equilibrium olivine.

equilibrium olivine. The effect of these changes on the composition of olivine can be estimated with the use of the COMAGMAT software package: for the parental magma ([53], Table 1) with an eutectic (*Ol* + *Pl*) melt at the transition from the QFM – 1 to QFM + 1 buffer, the olivine composition changes from 85.7 to 86.4 mol % *Fo*. Obviously, this effect cannot be determining for the compositional trend of the Dovyren dunites (Fig. 8).

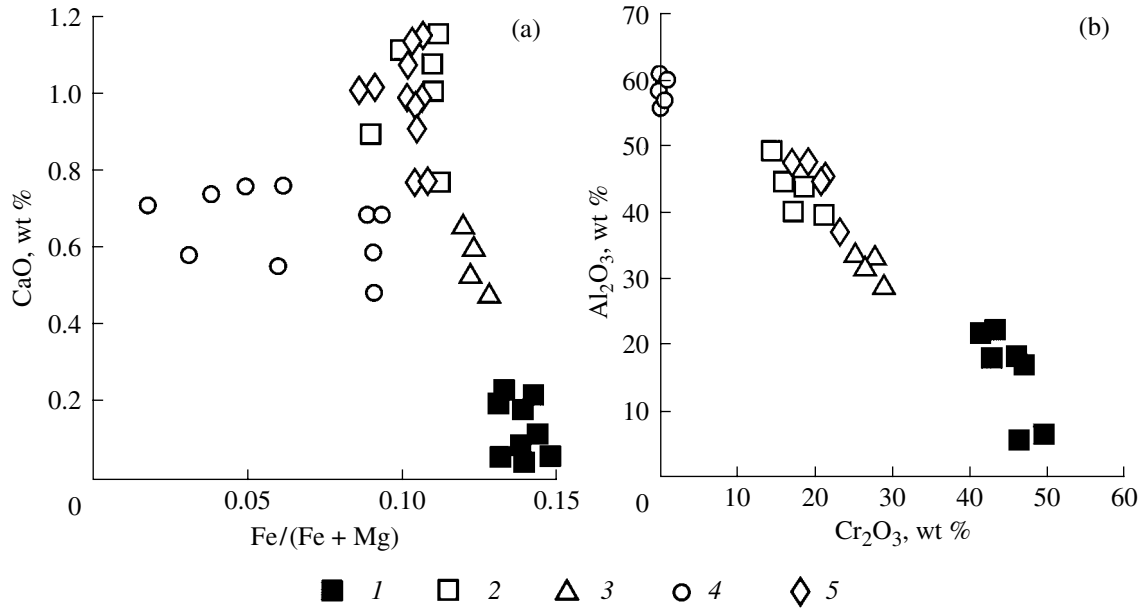

Fig. 9. Variations in the composition of (a) olivine and (b) Cr-spinel in ultramafic rocks and magnesian skarns of the Yoko–Dovyren Massif [23, 64].

Rock compositions: (*1*) uncontaminated dunites; (*2*) contaminated dunites; (*3*) reaction wehrlites; (*4*) magnesian skarns; (*5*) chromitites.

(3) An increase in the mg# of the olivine can result from the partial melting of the primary olivine cumulus with the compaction of the crystalline phase and pressing-out the newly formed melt. The results obtained by simulating equilibrium melting for the same starting composition [53] indicate that, regardless of the redox conditions, an increase in the mg# of cotectic olivine by 2 mol % of the forsterite end member requires the melting (dissolution in the liquid) of 8–9 wt % of this mineral. Thereby the data point of the melt "departs" from the olivine–plagioclase cotectic for a region oversaturated with olivine at 9.5 wt % MgO in the liquid. This effect can take place if two conditions are fulfilled.

In a dry system, one of the factors responsible for the melting of cumulates may be a temperature extremum, which appears near the lower solidification front and is related to the "burial" of a temperature distribution corresponding to the crystallization sequence of the magma in the mixture of crystals and melt (see Fig. 48 in [60]). With reference to large intrusions, this mechanism was first proposed by M.Ya. Frenkel' (personal communication in 1977) and was taken into account when our convection–accumulation model for differentiation was developed; this model did demonstrate that partial melting zones can develop at boundaries with olivine–plagioclase and olivine–plagioclase–augite cumulates [28]. An additional (and may be the determining) factor of the melting and subsequent recrystallization of primary olivine cumulates could be the accumulation of volatiles in the residual melt and an increase in the CO_2 pressure as a result of the associated crystallization of the magma and the assimilation of carbonate–terrigenous material.

Effects of the assimilation of carbonates. Evidence of carbonate decomposition and Ca passing into the magmatic melt is the occurrence of magnesian apocarbonate skarns in the Dovyren intrusion [16, 36], the high CaO concentration in high-Mg olivine from the units of contaminated dunites [23, 50], and the appearance of olivine pyroxenites or wehrlites in the upper portion of zone A [20, 21].

The Yoko–Dovyren Massif is hosted in a black shale sequence with a 140-m layer of dolomite, which approaches the lower contact of the pluton and can be traced in the form of separated blocks of magnesian skarn in the dunite (Fig. 3). The results of geological and experimental investigations show that spinel–brucite skarns in small apocarbonate xenoliths could be formed by the thermal decomposition of dolomite into the periclase + calcite + CO_2 association [50, 51]. The decarbonatization products mixed with the intercumulus melt and formed diopside and fassaite veins in the dunites. The CO_2 fluid released thereby could suppress the melting temperature of the olivine cumulate and increase the mg# of the residual melt and coexisting olivine. As is known from experimental data, the temperature of the olivine–melt equilibrium decreases by a few dozen degrees even at a low water concentration (a few tenths of a weight percent) [61, 62]. The effects of CO_2, Cl, and other volatile components were studied less thoroughly. Nevertheless, it is worth considering the effect of (H_2O)–CO_2 fluid and CaO dissolution on the expansion of the clinopyroxene field and an

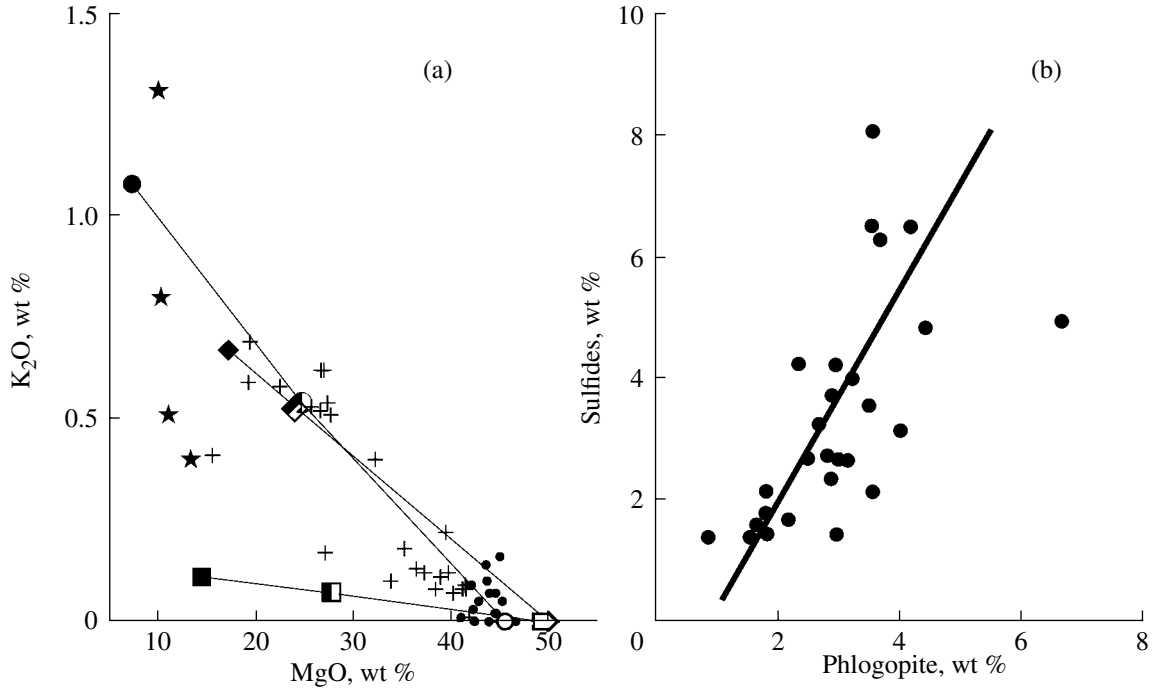

Fig. 10. (a) Trends of K_2O and MgO concentrations in LCZ rocks and (b) the correlation between the contents of phlogopite and sulfides in plagioperidotites (according to data from [72]).
See Fig. 8 for symbol explanations.

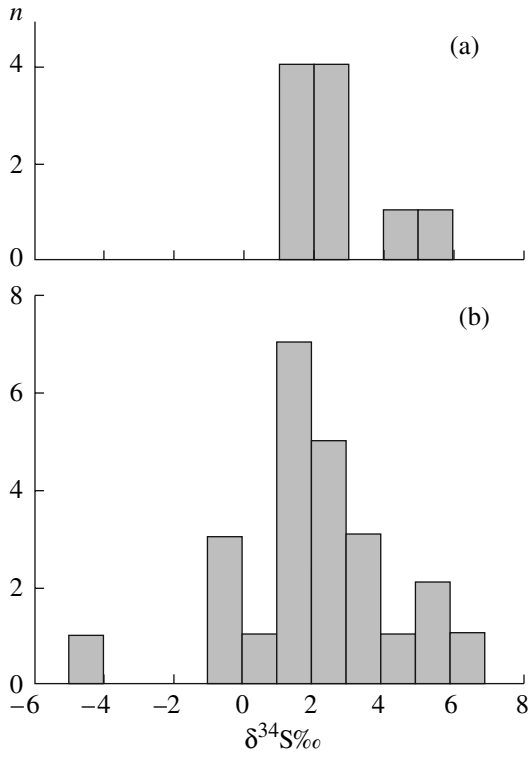

Fig. 11. S isotopic composition of (a) Cu–Ni sulfide ores and (b) low-sulfide platiniferous units of the Yoko–Dovyren Massif (according to data from [82]).

increase in the mg# of mafic phases in the Dovyren magma. This is confirmed by experimental data on the dissolution of carbonates in alkali basaltic magmas [63]. According to these authors, the melts dissolved 3–12 wt % carbonates at 1150–1050°C at a significant CO_2 emission from the system. This was associated with an increase in the mg# of the coexisting clinopyroxene and olivine owing to the dissolution of the calcite

$$CaCO_3(Carb) + 2SiO_2(l) + MgO(l) = CaMgSi_2O_6(Cpx) + CO_2\uparrow \quad (5)$$

and magnesite

$$2MgCO_3(Carb) + SiO_2\,(l) = Mg_2SiO_4\,(Ol) + CO_2. \quad (6)$$

components of dolomite. If the Dovyren magma contained ~30% olivine crystals and 70% melt, the complete dissolution of a 140-m carbonate layer in the central part of the massif (~3 km thick) results in the maximum scale of assimilation of 100 × 140/(0.7 × 3000) = 6.7%. It can be expected that this process could result in a unit of olivine–clinopyroxene rocks (high-Mg wehrlite) some 200 m thick.

An obvious effect of the dissolution of carbonates in the Dovyren magma was an increase in the Ca concentration in olivine [50]. Figure 9a shows the variations in the composition of olivine from the contaminated and uncontaminated dunites (according to [64]). The diagram demonstrates a pronounced trend in Ca enrichment and an increase in the mg# of the olivine, with the CaO concentration in olivine of the composition $Fo_{88–90}$

reaching 1 wt %. An important result of this analysis is the discovery of coupled variations in the composition of coexisting spinel in the ultramafites and chromitite lenses (Fig. 9b). An increase in the mg# and ca# of olivine is associated with a decrease in the Cr_2O_3 concentration and an increase in the al# of the spinel. This effect can likely be regarded as another important indication of the degree of parental magma contamination with carbonate material. In the context of the evaluation of parameters of the Dovyren magma (Table 1), it is worth mentioning the narrow compositional range of olivine from the uncontaminated dunite: $Fo_{85–87}$ (Fig. 9a). This suggests that the "dunite trend" in the FeO–MgO diagram is, in fact, compositional variations of the contaminated dunites.

Another indication of carbonate assimilation is likely the heavier oxygen isotopic composition of the olivine: $+8.1 \le \delta^{18}O \le 9.2‰$ [21, 65]. Intercumulus plagioclase in the dunites and cumulus plagioclase of the gabbronorites have compositions within the range of $+8.6 \le \delta^{18}O \le 9.4‰$. At the same time, olivine, clinopyroxene, and phlogopite from inner-contact rocks of the Yoko-Dovyren Massif show more stable characteristics: $+5.9 \le \delta^{18}O \le 6.4‰$, which are close to the mantle values [32, 66]. These values fall within the range of isotopic compositions determined for continental mafites and ultramafites, many of which (in contrast to those typical of MORB, which have $\delta^{18}O = 5.7‰$ on average) display an isotopically heavier oxygen composition: $\delta^{18}O = 6–8‰$ and higher. The possibility of obtaining heavier oxygen isotopic composition during the assimilation of mafite magmas with carbonates also follows from the results obtained on the Jinchuan intrusive complex in northern China [67]. According to these data, the CaO/Al_2O_3 ratio definitely shows a correlation with $\delta^{18}O$ in ultramafites from the inner parts of the massif ($\delta^{18}O \sim 5–6‰$) and in plagioperidotites and plagiodunites from the inner-contact zone ($\delta^{18}O \sim 10–11$) and marbles in contact with the intrusion ($\delta^{18}O$~16–19‰). The difference with the Dovyren intrusion is that the isotopic exchange was constrained there to the inner-contact zone.

It is interesting to consider the effect of carbonate assimilation on the conditions of melt saturation with S and on the possibility of sulfide segregation in decarbonatization zones [68]. Direct evidence of these processes is provided by the development of an aureole of disseminated sulfides around apocarbonate skarns in the Yoko–Dovyren Massif (see, for example, [21, 69]). It is reasonable to assume that CO_2 released during decarbonatization affected redox equilibria near the xenoliths, and this led to the partial oxidation of Fe^{2+} to Fe^{3+} and a decrease in the FeO concentration in the melt. It is thereby reasonable to expect that the S solubility should decrease and sulfide phases should crystallize from the melt (see, for example, [70, 71]). This mechanism has been discussed with reference to the genesis of disseminated and impregnated ores at the Jinchuan deposit [67].

The study of interactions between the Dovyren magma and carbonate xenoliths may shade light not only on the emplacement mechanisms of the Dovyren magma but also on certain details of the development of the layered massif that cannot be explained within the scope of simple crystallization fractionation [24, 25], as well as on the genesis of sulfides within the chamber.

Role of the assimilation of terrigenous rocks. The siltstones of the Ityka Formation hosting the pluton were affected by intense contact metamorphism. The thermal metamorphic aureole at the lower outer contact varies from 100–200 m in thickness at the southeastern margin of the massif to 400 m in its northwestern flank [16, 20]. Thermal metamorphism produced a hornfels succession of predominantly amphibole-hornfels facies, which gives way to pyroxene hornfels in contact with the massif. Simultaneously the SiO_2 concentration in the hornfels decreased from 67 to 60 wt % [21]. The plagioperidotites and associated sills ubiquitously contain minerals atypical of the lower part of the Layered Series: phlogopite and bronzite (large orthopyroxene oikocrysts serve as a reliable mapping guide, which makes these rocks different from the plagioclase lherzolites and plagiodunites). This is thought to be evidence that the parental magma actively interacted with the siltstone. The variations in the SiO_2 and K_2O concentrations in the plagioperidotites (Figs. 6, 8, 10) highlight the migration of these components from the terrigenous sediments into partly crystalline rocks in the bottom part of the intrusion [21]. This conclusion is, however, at variance with the plagioperidotite nature of the Dovyren magma, which implies that the weighted mean composition of the intrusion should correspond or at least be close to the average composition of the plagioclase lherzolites (see above). This problem can be resolved within the framework of the hypothesis of the selective migration of water and alkalis from the host sediments without their significant "bulk-rock" assimilation [21]. With regard to the above petrological data, these considerations should be revised.

The broad occurrence of phlogopite (± pargasite) in the plagioclase lherzolites suggests that water could be provided to the lower part of the Dovyren chamber by host siltstones when they were metamorphosed into hornfels [20, 21]. The contents of phlogopite and sulfides in the rocks of the LCZ are correlated with those in the bottom plagioperidotite sills (Fig. 10b). Such relations suggest genetic links between the segregation of sulfides and the large-scale metasomatic transformations of the plagioclase peridotites or the partly crystalline parental magma in the bottom part of the chamber. This is one of the key issues relating the role of the prechamber and intra-chamber genesis of the Ni sulfide ores in the course of the evolution of the Dovyren magma and the origin of the Yoko–Dovyren Massif.

The prechamber contamination of the parental magma Yoko-Dovyren intrusion. The problem was discussed starting at an early stage of the isotopic–

geochemical studies, when anomalous $^{87}Sr/^{86}Sr$ ratios were determined in the rocks of the massif: 0.712 on average [30, 73]. Certain traces of crustal contamination were revealed in the Sr–Nd systematics and the Pb isotopic composition [33]. According to these data, the $^{87}Sr/^{86}Sr$ ratio varies from 0.7101 to 0.7135 (for the isochron corresponding to 673 Ma) at $-16.3 \le \varepsilon_{Nd} \le -14.1$ variations. This is much lower than the parameters of the depleted mantle. The $^{207}Pb/^{204}Pb$ (15.477–15.501) and $^{208}Pb/^{204}Pb$ (37.17–37.59) ratios were very close to the hypothetical composition of the Archean–Late Proterozoic upper continental crust. According to Amelin et al. [33], these relations can be regarded not only as evidence of the contamination of the parental magma with crustal material but also, perhaps, as an indication of the existence of the enriched mantle beneath the Siberian craton in the Late Proterozoic, with this mantle generated with the participation of ancient subducted lithospheric material.

Pioneering results were recently obtained on the mineralogical and chemical composition of crystalline and melt inclusions in cumulus olivine and plagioclase from ultramafites of the Yoko–Dovyren Massif [31]. The abundance of haplogranite glassy inclusions in polyphase mineral inclusions can be explained by widespread reaction interactions between the parental magmas and crustal material and by the mixing of the hybrid products at various levels of the magmatic system (including the lower levels of the continental crust) as a result of the emplacement of fresh portions of parental melts from deeper levels [73]. These considerations are consistent with the concept according to which primitive magmas coming from the mantle are undersaturated with sulfides, but crustal contamination suppresses the S solubility in these liquids and triggers (and maintains) silicate–sulfide immiscibility [1, 74]. Such processes could play a determining role in the saturation of the parental magma in sulfides, and this magma served later as the source of disseminated and massive ores at the Baikal'skoe deposit [26]. The early saturation of the Dovyren magma in sulfides is consistent with the occurrence of sulfide inclusions in primitive olivine from the plagioperidotites and dunites [21]. At the same time, the recrystallization of melt inclusions with the development of olivine–amphibole aggregates and acid residual glasses in the inclusions could also result from the reequilibration of the primary inclusions with host olivine in the course of cooling after the entrapment of the inclusions [75].

SULFIDE MINERALIZATION AND ORE POTENTIAL

The Yoko–Dovyren Massif and small plagioclase peridotite bodies in the southeastern flank of the Synnyr rift structure host mineral deposits and occurrences of Cu–Ni sulfide, magmatic ore mineralization, and traces of noble-metal mineralization.

Cu–Ni sulfide ores were discovered in the Dovyren intrusion by M.M. Tetyaev in 1914 in the course of field traversing in the western Baikal territory. Exploration and prospecting operations and the evaluation of the resources of these occurrences were accomplished in the 1960s by the Buryat Geological Department of the Ministry of Geology of the Soviet Union. According to the results of this work, the resources of the Baikal'skoe deposit were classed with subeconomic (150000 tons) and with low-grade ores. Exploration operations at this territory resulted in the discovery of the Kholodnenskoe Cu–Zn sulfide deposit in the southeastern flank of the Synnyr structure and the Avkit Cu–Ni sulfide occurrence in the ore field of this deposit.

Sulfide mineralization at the Baikal'skoe deposit and Avkit mineral occurrence is related to bodies of plagioclase peridotites. These rocks compose the bottom zone of the Yoko–Dovyren Massif, and the plagioclase lherzolite sills approach it at an acute angle. These sills can be fragments of magma conduits that fed the intrusive chamber from below. Economic sulfide ores were found in the northeastern margin of the massif in the bottom plagioperidotites. Based on the core materials from the area of Shkol'nyi Stream (Ozernyi prospect) and observations in exposures at the surface, a vein was revealed that trends for 650 m and has a thickness of approximately 1 m [21]. The ores contain up to 2.1 wt % Ni, 0.64% Cu, 0.14% CoO, 0.2 ppm Pt, 0.68 ppm Pd, 0.02 ppm Rh, 0.14 ppm Au, and 10.7 ppm Ag. The massive ores are surrounded by an aureole of disseminated sulfide mineralization and are spatially constrained to numerous faults cutting across the peridotites. Bodies of the disseminated ores are also typical of the central and southwestern parts of the bottom zone and were traced for 200–1400 m along their strikes at a width of 2–25 m at the surface. These ores are of lower grade and contain 0.5 wt % Ni, 0.28% Cu, 0.03% CoO, 0.26 ppm Pt, 0.9 ppm Pd, 0.01 ppm Rh, 0.06 ppm Au, and 16.3 ppm Ag.

The massive ores consist of 40–95% hexagonal pyrrhotite and contain minor concentrations of troilite, pentlandite (7–25%), and chalcopyrite (0.1–6%). The minor minerals are cubanite, ilmenite, magnetite, and pyrite, and the ores occasionally contain mackinawite, titanomagnetite, sphalerite, and molybdenite. The disseminated ores differ from the massive and brecciated ones in containing magnetite as a major mineral, minor chromium spinel and sphalerite, and occasional bornite [21, 76].

Low-sulfide noble-metal mineralization was discovered in the early 1990s in the central part of the Dovyren Massif, near the boundary between troctolite and the cyclically layered olivine gabbro series [77, 78]. The mineralization is restricted to the taxitic gabbro unit that includes veins of gabbro-pegmatites and anorthosite schlieren and lenses. The thickness of the anorthosite bodies ranges from a few centimeters to 5 m, and they usually trend for no more than 40 m.

They are oriented conformably with the layering and compose en-echelon "drapes" in the taxitic unit approximately 300 m thick, with the unit traced by field traversing for 19 km and, judging from the topography, extends for approximately 1 km downward [79]. The anorthosite bodies contain lean (approximately 5%) disseminated sulfide mineralization (pyrrhotite, pentlandite, cubanite, chalcopyrite, heazlewoodite, godlevskite, talnakhite, and bornite) in association with noble-metal minerals. The total PGE content in anorthosites from the taxitic unit reaches approximately 10 ppm, including 1.33 ppm Pt, 4.91 ppm Pd, 0.06 ppm Rh, 0.008 ppm Os, 0.13 ppm Ir, 0.009 ppm Ru, and 3.24 ppm Au [80], with Pt dominating over Pd in practically all samples. Noble-metal minerals found in the anorthosites of the platiniferous unit are mostly intermetallic compounds: tetraferroplatinum, tulameenite, rustenburgite, moncheite, and zvyagintsevite [76, 81]. This testifies to a low fugacity of sulfide sulfur (f_{S_2}) during the origin of this type of mineralization.

Currently available data on the S isotopic composition comprise a few analyses of the sulfide ores and a more representative database for low-sulfide units of the Yoko–Dovyren Massif (Fig. 11). These data indicate that the average isotopic characteristics of the massive Cu–Ni ores and sulfides from the platiniferous unit are close, thus suggesting a juvenile source of S for both types of the ore mineralization. Broader variations in $\delta^{34}S$ in the rocks of the PGE unit (Fig. 11) can be explained as resulting from the migration of fluids removing SO_2 late during the solidification of the residual melt [82]. These conclusions should, however, be confirmed by more systematic studies of the variations in the S isotopic composition of sulfides in the vertical section and along the strike of the intrusion. It is pertinent to mention that sulfides should also be examined in the aureoles of the gabbro-diabase dikes and the supposedly comagmatic Synnyr volcanic rocks.

Possible ore potential of the Dovyren Massif. The evaluation of the sulfide ore potential of mafite–ultramafite intrusions is based on the application of certain empirical and theoretical criteria. The former were established as a result of the long-term exploration and prospecting practice at mineral deposits and include (1) the affiliation of the magmatic complexes to a metallogenic epoch and metallogenic province productive for Cu–Ni sulfide mineralization, (2) a favorable geodynamic environment, and (3) the "right" type of the magmatic association of the layered massifs.

It is well known that the Earth's evolutionary history included time intervals when processes generating certain minerals were highly productive. For Cu–Ni sulfide ores, the most favorable time was the Precambrian and Mesozoic. The great majority of all the known largest mineral deposits of Precambrian age were formed in their metallogenic epochs: in the Archean and in the Early and Late Proterozoic [83]. The Archean magmatic deposits were related mostly to komatiite magmatism (for example, Kambalda in Australia). The Early Proterozoic deposits were related to layered mafite–ultramafite massifs, which were derivatives of boninite-like magmas (intrusions of the Pechenga–Varzuga and Vetrennyi belts in Russia). The Late Proterozoic epoch was responsible for the generation of the Synnyr–Dovyren Complex and a number of widely known large mineral deposits in the United States and Canada (Duluth, Muscox, and Voisey's Bay) and in northern China (Jinchuan). According to recently obtained data [84], the Jinchuan deposit has an age most closely similar to that of the Dovyren intrusive complex (825 and 740 Ma, respectively).

Recent palispastic reconstructions conducted by Chinese geologists [85] have demonstrated that the Northern Chinese and Siberian platforms were neighboring in the Late Riphean (800–750 Ma) at the eastern margin of the Rhodinia paleocontinent, and both occurred within the influence zone of an subequatorial superplume. The effect of this superplume can likely explain the breakup of Rhodinia in the Riphean and ultramafite magmatism in the marginal parts of both platforms. This geodynamic environment, which implies rifting and related mafic magmatism, was favorable for the generation of significant resources of sulfide mineralization [1, 2]. The restriction of the Yoko–Dovyren Massif and Avkit intrusion to flanks of the Synnyr rift structure and similarities in the petrochemistry of diabase sills in the Dovyren pluton and Synnyr volcanic rocks (Fig. 2) suggest genetic links of these intrusive bodies with the development of the Late Riphean rift in the margin of the Eastern Siberian craton.

Petrological and geochemical analogies of the Baikal'skoe and Jinchuan deposits. The genesis of the Jinchuan deposit in north central China is also thought to be related to Late Riphean rifting [84, 86], which resulted in the opening of an oceanic basin (the Paleoasian Ocean [87]) during the breakup of Rhodinia. Similarities in the age and geotectonic setting of the Dovyren and Jinchuan Ni-bearing complexes is empasized by their petrological–geochemical and metallogenic similarities (Table 2). Table 2 summarizes the principal characteristics of these deposits, which are analogous (in spite of the multifold difference in the resources of their Ni sulfide ores), with ranges of most of their parameters overlapping. In comparing their geological–tectonic characteristics, it should be taken into account that the broadly known concept of the geological setting of Jinchuan was recently revised (according to this concept, the major intrusions of this complex are subvertical mafite–ultramafite bodies that show traces of horizontal layering in the eastern block [58, 86]). The authors of [67, 88] presented geological arguments testifying that the intrusions of the Jinchuan Complex in their original setting were (similar to Dovyren) a single subtabular body, which was later affected by rotational tectonic deformations and metamorphosed to the greenschist facies.

Table 2. Comparison of geological characteristics and petrological–geochemical parameters of the Baikal'skoe and Jinchuan deposits

Characteristics of deposits	Baikal'skoe deposit (Yoko–Dovyren Massif)	Jinchuan
	Geological–tectonic setting	
Geological setting	Rift in a continental margin	
Age	PR_2 (R_3, ~740 Ma)	PR_2 (R_3, 825 Ma)
Type of association (primary form)	Dunite–troctolite–gabbro–norite layered massifs (subtabular body)	Ultramafite massifs (perhaps, a sill)
Evidence of assimilation of carbonates	Apocarbonate magnesian skarns	Apocarbonate magnesian skarns
	Petrological parameters	
Predominant rocks of the massifs	Plagioclase peridotites, dunites, troctolites, and gabbronorites	Lherzolites (70–80%), dunites, and olivine pyroxenites: all are olivine and chromite cumulates
Conditions of parental magma emplacement	P = 0.5–1 kbar, ~WM buffer, T = 1200–1250°C	P = 2–3 kbar, solidification temperature was 900–1050°C
MgO in melt (wt %)	7.5–10 %	~12%
Fo in olivine (mol %)	85–87	85.5
	Isotopic–geochemical features	
La/Lu (in intrusion)	4.5–9.3	4–10
$\delta^{18}O$	5.9–6.4	5–6
$^{87}Sr/^{86}Sr$	0.712 (average)	0.7091–0.7169
$^{143}Nd/^{144}Nd$	0.511464–0.511744	0.511772–0.511942
ε_{Nd}	from –16.3 to –14.1	from –8.9 to –12.0
	Metallogenic characteristics and sulfides	
Ni/Cu disseminated ores	1.8	1.5–1.7
Sum of PGE + Au	≤1.5 ppm	≤1.8 ppm
$\delta^{34}S$ in ores.	from + 1.1 to + 5.6	from –2 to +5
Sulfide inclusions	In olivine and chromite	In olivine and chromite

Note: Data on the Jinchuan deposit are compiled from [1, 58, 67, 84, 88–90] and the review [91].

An important geological feature of Dovyren and Jinchuan is their heterogeneous character and enrichment in olivine phenocrysts. Similar to data in [22] on the Dovyren pluton, the authors of [58] state that intratelluric olivine in the Jinchuan magma contained approximately 85 mol % of the forsterite minal, although this mineral crystallized from a more magnesian melt that contained close to 12 wt % MgO (Table 2). A mafic but not picrite–komatiite composition of the initial melt of both intrusive complexes follows from the relatively low Ni/Cu concentrations in the disseminated ores: Ni/Cu = 1.8 for Dovyren [21] and 1.5–1.76 for Jinchuan [86]. Such values of this ratio are typomorphic of sulfide settling from a liquid of basalt or gabbronorite composition [1]. This also follows from the weighted mean Ni/Cu = 0.92, which was calculated for a representative vertical section of the Yoko–Dovyren Massif characterized by 113 rock analyses [92].

The analogies mentioned above may be appended with similarities in the isotopic–geochemical signals in the Dovyren and Jinchuan rocks (see Table 2 for their $^{87}Sr/^{86}Sr$ and ε_{Nd} values), which suggest lower crustal contamination [26, 31, 67] and/or the anomalously enriched Riphean mantle from which the parental magmas were derived [33, 84]. The possibility of the assimilation of granitic material in the lower crust makes it possible to admit the relatively early, prechamber saturation of the initial melts with S. This is confirmed by the occurrence of sulfide inclusions in the primitive olivine and chromite. At the same time, uncertain issues for both complexes are the scale of carbonate assimilation during the filling of the magmatic chambers and the effect of these processes on the S solubility in the melts and the possibility of additional settling of sulfides in the chambers [50, 67].

Geological–petrological data on the Dovyren intrusive complex and metallogenic and geochemical analogies with the rocks of Jinchuan as one of the largest Ni sulfide deposits suggest positive outlooks for economic Cu–Ni–noble metal ore mineralization at Dovyren. The analysis of available geological–geophysical materials indicates that the Dovyren mineralized zone and the massif itself are still poorly explored [93]. The zone of Cu–Ni ore mineralization discovered in the 1960s trends for approximately 20 km and was examined only

fragmentarily, at a few exposed occurrences and to depths of 200–750 m in a thin network of boreholes. Deep-charge and gravimetric data in combination with VES-IP results, make it possible to predict high-grade sulfide ores in the deep ultramafites of the Yoko–Dovyren massif [93]. An increment of the resources can be expected as a result of the follow-up exploration of the flanks and deep levels of the Baikal'skoe deposit.

CONCLUSIONS

The review of petrological–geochemical data on the Yoko–Dovyren Massif presented above highlights important relations between the genetic interpretations of the inner structure of the massif and certain geochemical aspects linked to the analysis of the nature of the Ni sulfide mineralization and the evaluation of the possible ore potential.

The **key problem** here is the evaluation of the temperature and composition of the initial melt and the chemical and modal composition of the parental magma. COMAGMAT simulations in application to the inverse [22] and forward [28, 29] problem of the modeling of natural intrusive bodies demonstrate that the Dovyren magma contained abundant intratelluric olivine (20–50%) when injected into the chamber, with this olivine having the composition $Fo_{85–91}$ (Table 1). These characteristics imply broad variations in the temperature (1185–1400°C) and MgO concentration in the initial melt (~7.5–17 wt %). This scatter results in a significant uncertainty of the estimates for the sulfide content in the Dovyren magma. Experimental results demonstrate that the temperature, composition, and reduction of magmatic melts control the S solubility in them and the conditions under which sulfide phases crystallize and/or dissolve [70, 71, 94–100]. If, presumably, the lithostatic pressure in the Dovyren chamber was close to 1 kbar and the redox conditions corresponded to the wustite–magnetite (WM) buffer, then, for a melt of gabbronorite composition at a temperature close to 1200°C [22], the S solubility should be approximately 0.10–0.11 wt %, and picrite–komatiite melts at 1350–1400°C [28, 29] may contain 0.19–0.25 wt % S. [4] This precludes an unambiguous evaluation of the degree of the under- or oversaturation of the Dovyren magma with sulfides.

The average S content in plagioperidotites of the massif is 0.12 ± 0.06 wt % [21]. Assuming a minimum estimate of 0.06 wt % S (for the minimum content of sulfide in these rocks) and ~40% intratelluric olivine phenocrysts in the plagioperidotite magma, we arrive at an estimate of 0.10 wt % S in this liquid. The comparison of our estimates for the S solubility and this "real" S concentration in the melt leads to principally different conclusions: for the relatively low-temperature gabbronorite melts, it is reasonable to assume that the initial magmatic material was saturated with sulfides, whereas the picrite–komatiite system should have been significantly undersaturated in sulfides. This results in differences in the genetic schemes and evaluations for the scale of sulfide settling in the chamber. The first situation implies the predominant segregation of primary magmatic sulfides (perhaps, with an addition of a certain amount of "chamber" sulfide S), whereas the second situation suggests in situ crystallization and accumulation of sulfides as a result only of the assimilation of the host rocks by the magma. The problem can be solved based on a complex approach, with a combination of precise geochemical investigations of the rocks, minerals, and inclusions and with the simulation of phase equilibria in the crystallizing magma with regard for the segregation of sulfide phases [12, 101].

Parameters of the parental magma can be specified based on the identification and interpretation of "anomalous" petrochemical trends for the lower contact [37] and reversal [38] zone of the pluton (Fig. 4). Models taking into account crystal accumulation at the lower solidification front (Fig. 6) and cumulus compaction (Fig. 7) suggest the inevitable generation of such trends with an increase in the content of cumulus olivine and MgO in the vertical section of the rocks up from the lower inner contact. These trends correspond to mixing lines of intratelluric olivine and the initial magmatic liquid and thus impose rigid constraints on the compositions of the initial olivine and melts as end components (Fig. 8). Graphical reconstructions with the use of olivine control lines in combination with data on the compositions of minerals from the uncontaminated dunites (Fig. 9) indicate that parental magma of the Yoko–Dovyren pluton came to the chamber which contained olivine with no more than 87 mol % of the forsterite end member. These evaluations constrain the possible temperature range of the parental magma to 1200–1250°C, and its crystallinity during emplacement is, thus, constrained to 35–50%, with this information needed to calculate the effective viscosity and density of the initial suspension. The exact geological knowledge of properties of a magmatic system is required to develop models for the separation and concentration of sulfide globules in the magma conduit and chamber [102, 103].

A closed chamber or a flowing system? Estimates of the temperature and composition of an initial melt by geochemical thermometry are independent of the emplacement mechanism of the melt and the succession of the chamber filling with the magma and its subsequent differentiation [12]. Evaluations of the modal composition of the parental magma, including the content of olivine phenocrysts, are based on data on the distribution of major elements in vertical sections and the weighted mean composition of the intrusions [13]. The latter approach implies a single act of magma emplacement into a closed chamber and the absence of other magma injections and magma feeders. Assuming the constancy of the bulk composition of the emplaced

[4] Calculations by the model for S solubility [101].

material leads to the contradiction that arises when thermodynamic simulations are made for the Yoko–Dovyren Massif [22]. Thermometric data on primitive rocks point to a gabbronorite composition of the initial melt, whereas calculations for the high-Mg average composition of the massif at temperatures of ≤1200°C yielded high concentrations of an intratelluric phase (75–80%) and an extremely low content of the complementary magmatic liquid (20–25%). This inconsistency can be eliminated if the chamber is regarded as an open system through which much more basite magma had flowed early in the course of the evolution of the massif than it can be assumed based on the volume of the gabbroids, gabbronorites, and norites in the upper part of the Yoko–Dovyren Massif. In this situation, it is reasonable to relate the origin of the dunite sequence to the cooling history of the olivine cumulates, which were produced by the settling of excess subcotectic olivine ($Ol \pm Pl$) from the magma that flowed through the chamber and whose composition corresponded to olivine gabbronorite. This approach makes it possible to interpret the Dovyren chamber as an intermediate magma conduit from which much of the initial melts (and perhaps, also their derivatives) were removed. Indirect evidence in support of this concept is the wide occurrence of gabbronorite sills and dikes around the Dovyren Massif and the strong predominance of basaltic andesites and andesites among the supposedly comagmatic Synnyr volcanic rocks. The interpretation of the Dovyren chamber as a temporal magma conduit makes it possible to explain the insignificant variations in the chemistry of the rock-forming minerals in uncontaminated rocks in the lower part of the vertical section at the contrasting modal layering of the massif (Fig. 5). To simulate these features within the scope of the convection–accumulation model, Bolikhovskaya et al. [29] had to assume free convection and the reequilibration of minerals in the highly crystalline suspensions. Thereby the modeled bodies evolved not according to the fractional crystallization mechanism but in compliance with a mechanism close to the equilibrium crystallization of residual systems with abundant suspended olivine crystals. The model of an intermediate magmatic chamber seems to be advantageous from the physical viewpoint, because it does not require the existence of hydrodynamically unstable suspensions for a long time. This interpretation implies that the Dovyren chamber was "closed" only after a significant volume of gabbronorite magma passed through it and a certain amount of olivine has been settled out. A differentiation process according to the convection–accumulation mechanism with the development of clearly pronounced compositional layering more probably affected the upper part of the magmatic reservoir. This alternative to the genesis of the Yoko–Dovyren Massif as an originally "closed" intrusive body deserves a detailed petrological analysis.

Another important problem of Dovyren is the occurrence of much dunite in the vertical section, with these rocks containing highly magnesian olivine (87–92 mol % *Fo*, i.e., higher than in the initial plagioperidotite magma) [22, 33, 55]. The authors of this review arrived at the conclusion that this resulted from the partial melting and compaction of the primary olivine cumulates in response to the infiltration of intercumulus melt enriched in volatiles. The volatile components were likely provided mostly by carbonate xenoliths, whose thermal decomposition brought about an increase in the CO_2 pressure and the transfer of the calcite–magnesite components into the melt. This follows from (1) the occurrence of apocarbonate magnesian skarns [16, 36], (2) high CaO concentrations in olivine from the contaminated dunites [23, 50], (3) the appearance of olivine pyroxenites and wehrlites in the upper part of the dunite zone [20, 21], (4) correlations between olivine and chromite compositions in the contaminated and uncontaminated dunites [64], (5) broad variations in the oxygen isotopic composition of olivine and plagioclase from rocks of the Layered Series [32, 65, 66], (6) experimental data on the dissolution of carbonates in alkali basaltic melts [63], and (7) analogies of the isotopic–geochemical characteristics of the rocks with those of rocks from the Jinchuan ultramafic complex [67].

The **anomalously high Sr and low Nd isotopic ratios** and the Pb isotopic composition of rocks from the Yoko–Dovyren Massif [30, 33, 35] seem to suggest a hybrid nature of the Dovyren magma, which was produced by the interaction of primary mantle melts with the granulite layer in the lowermost continental crust. Indirect evidence of the action of these processes is provided by the abundance of acid melt and polyphase crystalline inclusions in olivine from the dunite zone [31]. This hypothesis looks appealing in light of the felsitization concept [1, 74] as the main reason for the saturation of the Dovyren magma with sulfides. At the same time, another alternative is proposed by the hypothesis of the melting of anomalously enriched mantle material that occurred beneath the Siberian craton in the Late Proterozoic [33].

Geological–petrological genetic model for the Synnyr–Dovyren Complex. We consider the results presented above to be the basis for a genetic scheme relating the genesis of volcanic rocks of the Synnyr rift, Dovyren intrusive complex, and Baikal'skoe Cu–Ni–PGE deposit (Fig. 1). This scheme implies that the picrite–komatiite parental melts were formed in the upper (likely enriched) mantle and were contaminated at the lowest levels of the continental crust with the development of suspensions of less magnesian sulfide-saturated melt and olivine (~$Fo_{87–88}$) crystals. Magma differentiation during its ascent and reactive interactions with the host rocks within the second structural floor in the Synnyr depression gave rise to sills of plagioclase lherzolites (olivine : melt ~ 1 : 1) and comagmatic diabase dikes (olivine << melt), which crystallized from a mixture of gabbronorite melt and olivine (~$Fo_{85–87}$) at temperatures of 1200–1250°C. The Yoko–

Dovyren pluton can be regarded as a crystallization product of plagioperidotite magma (olivine + gabbronorite melt) in a large chamber, which initially was an intermediate chamber for the Synnyr volcanic rocks. The culmination of these processes was subaerial volcanism of contrasting type (Inyaptuk Formation) with indications of the contamination of the parental magmas with continental lithospheric material (microxenoliths of garnet gneisses in acid lavas), which gave way to subaquatic eruptions of basaltic andesite lavas (Synnyr Formation). The upper crustal assimilation of the host terrigenous–carbonate rocks facilitated an additional decrease in the S solubility in the Dovyren magma, the crystallization and accumulation of finely dispersed sulfides in the near-mouth part of the magma conduit (perhaps, at the northeastern termination of the massif), plagioperidotites of the lower zone and in the southwestern flank of the intrusion. Conceivably, this situation resembles the situation with the development of the Voisey's Bay sulfide deposit in Labrador, where major occurrences of Cu–Ni sulfide ores are restricted to swellings in the magma conduits during magma transfer from the lower to upper chambers [7, 9, 104]. Erosion and subsequent tectonic deformations did not expose the main orebodies of the Yoko–Dovyren Massif. The ores were exposed only as single lenses of massive ore and parts of the mineralized marginal zone with disseminated mineralization.

The aforementioned conclusion should not be regarded as a rigorous prediction of economic mineralization because it does not include evaluations of the reserves. In fact, this is merely a statement that the structure of the pluton and the composition of its rocks and rare orebodies show a set of petrochemical and mineralogical characteristics that fit known genetic features of Ni sulfide deposits [1]. The newly discovered criteria include estimates of the solubility of sulfide S in the initial melts [101] and the application of this information to characterizing the possible volumes of sulfide ores in the unexposed part of the massif. Indeed, if the average S concentration in the plagioclase lherzolites (0.12 wt %) is no lower than in deep peridotites and a realistic evaluation is available for the S solubility in the initial gabbronorite melt (~0.10 wt %), one can calculate the minimum amount of sulfides that could be segregated from the sulfide phase suspended in the melt. For this purpose, we can, again, use the assumption of ~40% olivine (+ sulfide) crystals in the plagioperidotite material. Then, from the mass balance for S $0.12 = 37f_S + 0.6 \times 0.10$, we obtain $f_S = (0.12–0.6 \times 0.10)/37 \sim 0.0016$, where f_S is the average weight percentage of sulfides disseminated in the parental magma (0.16 wt %), and the value of 37 wt % is close to the S concentration in the stoichiometric pyrrhotite FeS. Let us now assume that the LCZ plagioperidotites account for 5 vol % of the intrusive body (this is the minimum estimate under the assumption of the thickness of the plagioclase lherzolites in the central part of approximately 150 m). Using the evaluated volume of the Yoko–Dovyren Massif of 350 km^3 and the density of peridotite of ~3 g/cm^3, we obtain a minimum estimate for the mass of these contact ultramafites, including the unexposed part: $350 \times 0.05 \times 3 \times 10^{15}$ g = 52.5×10^{15} g. Hence, the total mass of the potentially "cumulus" sulfide phase concentrated in the plagioclase peridotite unit is $52.5 \times 10^{15} \times 0.0016$ g = 0.084×10^{15} g = 8.4×10^7 tons or 84 million tons. Assuming that no more than 1% of these sulfides formed the orebodies, we arrive at an estimate of approximately 0.8 million tons in recalculation to pure pyrrhotite or close to 4 million tons of rich disseminated ores with 20% sulfides. This is more than one order of magnitude greater than the resources of Ni sulfide ores evaluated based on exploration data (see above). Note that this estimate does not take into account the possibility of the additional crystallization of sulfides in the simultaneous processes of chamber differentiation and the assimilation of carbonate–terrigenous material.

Irrespective of the validation or invalidation of this prediction of economic ore mineralization, studies of the Synnyr–Dovyren volcanic–plutonic complex are of fundamental significance for the development of genetic models for Ni sulfide ores. The further study of the inner structure, mineralogy, and composition of rocks composing the Yoko–Dovyren Massif with the application of modern petrological–geochemical techniques will place this intrusion among world-class structures in terms of genetic importance. The results of these studies can be applied in developing new prospecting guides and criteria for the evaluation of resources of base- and noble-metal sulfide ores in less thoroughly explored mafite–ultramafite complexes in eastern Siberia.

ACKNOWLEDGMENTS

We thank A.V. Lavrenchuk for comments on our simulation results by the convection–compaction model of differentiation and E.V. Koptev-Dvornikov for the elucidation of certain issues concerning "assembling" the generalized vertical section of the Yoko–Dovyren Massif.

This study was carried out under the Cooperation Agreement between the Vernadsky Institute of Geochemistry and Analytical Chemistry, Russian Academy of Sciences, and the Centre for Ore Deposit Research (CODES), University of Tasmania in Hobart, Australia, and was financially supported by the Russian Foundation for Basic Research, project no. 08-05-00194.

REFERENCES

1. A. J. Naldrett, *Magmatic Sulfide Deposits of the Copper–Nickel and PGE Ores* (SPBGU, St. Petersburg, 2003) [in Russian].
2. A. P. Likhachev, *PGE–Copper–Nickel and PGE Deposits* (Eslan, Moscow, 2006) [in Russian].

3. A. J. Naldrett, P. C. Lightfoot, V. Fedorenko, et al., "Geology and Geochemistry of Intrusions and Flood Basalts of the Noril'sk Region, USSR, with Implications for the Origin of the Ni–Cu Ores," Econ. Geol. **87**, 975–1004 (1992).
4. C. Li, E. M. Ripley, and A. J. Naldrett, "Compositional Variations of Olivine and Sulfur Isotopes in the Noril'sk and Talnakh Intrusions, Siberia: Implications for Ore-Forming Processes in Dynamic Magma Conduits," Econ. Geol. **98**, 69–86 (2003).
5. N. T. Arndt, G. K. Czamanske, R. J. Walker, et al., "Geochemistry and Origin of the Intrusive Hosts of the Noril'sk–Talnakh Cu–Ni–PGE Sulfide Deposits," Econ. Geol. **93**, 495–515 (2003).
6. V. A. Rad'ko, "Model of Dynamic Differentiation of the Intrusive Traps of the Siberian Platform," Geol. Geofiz., No. 11, 19–27 (1991).
7. A. J. Naldrett, "Key Factors in the Genesis of Noril'sk, Sudbury, Jinchuan, Voisey's Bay and Other World-Class Ni–Cu–PGE Deposits: Implications for Exploration," Aust. J. Earth Sci. **44**, 283–315 (1997).
8. A. J. Naldrett, "World-Class Ni–Cu–PGE Deposits: Key Factors in Their Genesis," Miner. Deposita **34**, 227–240 (1999).
9. W. D. Maier, C. Li, and S. A. De Waal, "Why Are There No Major Ni–Cu Sulfide Deposits in Large Layered Mafic–Ultra-Mafic Intrusions?," Can. Mineral. **39**, 547–556 (2001).
10. A. V. Sobolev, "Melt Inclusions in Minerals as a Source of Principle Petrological Information," Petrologiya **4** (3), 228–239 (1996) [Petrology **4**, 209–220 (1996)].
11. L. V. Danyushevsky, F. N. Della-Pasqua, and S. Sokolov, "Re-Equilibration of Melt Inclusions Trapped by Magnesian Olivine Phenocrysts from Subduction-Related Magmas: Petrological Implications," Contrib. Mineral. Petrol. **138**, 68–83 (2000).
12. A. A. Ariskin and G. S. Barmina, *Modeling of Phase Equilibria during Crystallization of Basaltic Magmas* (Nauka, Moscow, 2000) [in Russian].
13. A. A. Ariskin and G. S. Barmina, "COMAGMAT: Development of a Magma Crystallization Model and Its Petrologic Applications," Geochem. Int. **42** (Suppl. 1), 1–157 (2004).
14. E. G. Distanov, K. R. Kovalev, R. S. Tarasova, et al., *Kholodninskoe Sulfide–Base Metal Deposit in the Precambrian of the Baikal Region* (Nauka, Moscow, 1982) [in Russian].
15. N. L. Dobretsov, A. A. Melyakhovetskii, I. V. Ashchepkov, et al., *Structural–Metamorphic Criteria of Metamorphogenic Mineralization* (Nauka, Novosibirsk, 1987) [in Russian].
16. S. A. Gurulev, *Geology and Formation Conditions of the Yoko–Dovyren Gabbro–Peridotite Massif* (Nauka, Moscow, 1965) [in Russian].
17. M. M. Manuilova and V. V. Zarubin, *Precambrian Volcanogenic Rocks of the Northern Baikal Region* (Nauka, Leningrad, 1981) [in Russian].
18. S. A. Gurulev, *Conditions of Formation of Basic Layered Intrusions* (Nauka, Moscow, 1983) [in Russian].
19. P. A. Balykin, G. V. Polyakov, V. I. Bognibov, and T. E. Petrova, *Proterozoic Basic–Ultrabasic Complexes of the Baikal–Stanovoy Area* (Nauka, Novosibirsk, 1986) [in Russian].
20. E. G. Konnikov, *Precambrian Ultrabasic–Basic Differentiated Complexes of Transbaikalia* (Nauka, Novosibirsk, 1986) [in Russian].
21. E. V. Kislov, *Yoko–Dovyren Layered Massif* (Izd. BNTs SO RAN, Ulan-Ude, 1998) [in Russian].
22. A. A. Ariskin, E. G. Konnikov, and E. V. Kislov, "Modeling of the Equilibrium Crystallization of Ultramafic Rocks with Application to the Problems of Formation of Phase Layering in the Dovyren Pluton, Northern Baikal Region, Russia," Geokhimiya, No. 2, 131–155 (2003) [Geochem. Int. **41**, 107–129 (2003)].
23. E. V. Pushkarev, S. L. Votyakov, I. S. Chashchukhin, and E. V. Kislov, "Olivine–Chromspinel Oxythermobarometry of Ultramafic Rocks of the Ioko–Dovyren Layered Massif," Dokl. Akad. Nauk **395**, 108–112 (2004) [Dokl. Earth Sci. **395**, 266–270 (2004)].
24. A. A. Yaroshevskii, D. A. Ionov, Yu. V. Mironov, et al., "Petrography and Geochemistry of the Yoko–Dovyren Dunite–Troctolite–Gabbbro–Norite Layered Massif (Northern Baikal Region)," in *Petrology and Ore Potential of Natural Rock Associations* (Nauka, Moscow, 1982), pp. 86–117 [in Russian].
25. A. A. Yaroshevskii, S. V. Bolikhovskaya, and E. V. Koptev-Dvornikov, "Geochemical Structure of the Yoko–Dovyren Layered Dunite–Troctolite–Gabbro–Norite Massif, Northern Baikal Area," Geokhimiya, No. 10, 1027–1039 (2006) [Geochem. Int. **44**, 953–964, (2006)].
26. E. G. Konnikov, V. S. Kovyazin, E. M. Prasolov, et al., "Petrological Formation Conditions of Sulfide Ores in the Mafic–Ultramafic Complexes," in *Ultramafic–Mafic Complexes of Precambrian Folded Areas* (Izd. BNTs SO RAN, Ulan-Ude, 2005), pp. 156–158 [in Russian].
27. P. A. Balykin, Doctoral Dissertation in Geology and Mineralogy (Novosibirsk, 2002).
28. A. V. Lavrenchuk, "Cumulative–Compaction Mode of the Formation of Layered Intrusions with Reference to the Yoko–Dovyren Massif," in *Proceedings of International Conference on Current Problems of Ore Formation and Metallogeny* (GEO, Novosibirsk, 2006), pp. 132–133 [in Russian].
29. S. V. Bolikhovskaya, A. A. Yaroshevskii, and E. V. Koptev-Dvornikov, "Simulation of the Geochemical Structure of the Ioko–Dovyren Layered Intrusion, Northwestern Baikal Area," Geokhimiya, No. 6, 579–598 (2007) [Geochem. Int. **45**, 519–537 (2007)].
30. E. V. Kislov, E. G. Konnikov, V. F. Posokhov, and V. L. Shalagin, "Isotopic Evidence for Crustal Contamination in the Yoko–Dovyren Massif," Geol. Geofiz., No. 9, 140–144 (1989).
31. E. G. Konnikov, S. V. Kovyazin, A. N. Nekrasov, and S. G. Simakin, "Interaction of Magmatic Fluids and Mantle Magmas with Lower Crustal Rocks: Evidence from Inclusions in the Minerals of Intrusions," Geokhimiya, No. 10, 1–20 (2005) [Geochem. Int. **43**, 939–958 (2005)].
32. E. V. Kislov, V. E. Vetshtein, and E. G. Konnikov, "Oxygen and Hydrogen Isotopic Composition of the Rocks of the Yoko–Dovyren Massif (Northern Baikal Region)," Geol. Geofiz., No. 5, 88–92 (1991).

33. Yu. V. Amelin, L. A. Neymark, E. Yu. Ritsk, and A. A. Nemchin, "Enriched Nd–Sr–Pb Isotopic Signatures in the Dovyren Layered Intrusion (Eastern Siberia, Russia): Evidence for Contamination by Ancient Upper-Crustal Material," Chem. Geol. **129**, 39–69 (1996).
34. E. G. Konnikov, E. V. Kislov, and A. A. Tsygankov, "Formation Types of the Nickel-Bearing Ultramafic Rocks of the Northern Baikal Region," Geol. Rudn. Mestorozhd. **29** (6), 38–45 (1987).
35. L. A. Neimark, E. Yu. Rytsk, B. M. Gorokhovskii, et al., "Lead Isotopic Composition and Genesis of the Lead–Zinc Mineralization of the Olokit Zone of the Northern Baikal Region," Geol. Rudn. Mestorozhd. **33** (6), 34–49 (1991).
36. N. N. Pertsev and L. I. Shabynin, "Skarn, Carbonate, and Brucite Xenoliths of the Yoko–Dovyren Massif," in *Contact Processes and Mineralization in the Gabbro-peridotite Intrusions* (Nauka, Moscow, 1979), pp. 85–96 [in Russian].
37. M. Ya. Frenkel', A. A. Yaroshevskii, A. A. Ariskin, et al., *Dynamics of the Chamber Differentiation of Basic Magmas* (Nauka, Moscow, 1988) [in Russian].
38. R. M. Latypov, "The Origin of Basic–Ultrabasic Sills with S-, D-, and I-Shaped Compositional Profiles by In-Situ Crystallization of a Single Input of Phenocryst-Poor Parental Magma," J. Petrol. **44**, 1619–1656 (2003).
39. M. Ya. Frenkel' and A. A. Yaroshevskii, "Crystallization Differentiation of Intrusive Magmatic Melt: Mathematical Modeling of Thermal Evolution and Differentiation of a Tabular Intrusion with Allowance for the Settlement of Solid Phases," Geokhimiya, No. 5, 643–668 (1978).
40. E. V. Koptev-Dvornikov, A. A. Yaroshevskii, and M. Ya. Frenkel', "Crystallization Differentiation of Intrusive Magmatic Melt: Estimation of Feasibility of the Sedimentation Model," Geokhimiya, No. 4, 488–508 (1979).
41. A. R. McBirney, "The Skaergaard Intrusion," in *Layered Intrusions* (Elsevier, 1996) Development Petrol. **15**, 147–180 (1996).
42. G. S. Nikolaev and A. A. Ariskin, "Burakovo–Aganozero Layered Massif in the Trans-Onega Area: II. Structure of the Marginal Series and the Estimation of the Parental Magma Composition by Geochemical Thermometry Techniques," Geokhimiya, No. 7, 712–732 (2005) [Geochem. Int. **43**, 646–665 (2005)].
43. S. J. Barnes, "The Effect of Trapped Liquid Crystallization on Cumulus Mineral Compositions in Layered Intrusions," Contrib. Mineral. Petrol. **93**, 524–531 (1986).
44. C. I. Chalokwu and N. K. Grant, "Reequilibration of Olivine with Trapped Liquid in the Duluth Complex, Minnesota," Geology **15**, 71–74 (1987).
45. G. S. Barmina, A. A. Ariskin, E. V. Koptev-Dvornikov, and M. Ya. Frenkel', "Experience in Estimating of Compositions of Primary Cumulus Minerals in the Differentiated Traps," Geokhimiya, No. 8, 1108–1119 (1988).
46. M. T. Mangan and B. D. Marsh, "Solidification Front Fractionation in Phenocryst-Free Sheet-Like Magma Bodies," J. Geol. **100**, 605–620 (1992).
47. B. D. Marsh, "Solidification Fronts and Magmatic Evolution," Mineral. Mag. **60**, 5–40 (1995).
48. S. Tait and C. Jaupart, "The Production of Chemically Stratified and Adcumulate Plutonic Igneous Rocks," Mineral. Mag. **60**, 99–114 (1996).
49. E. G. Konnikov, A. A. Ariskin, G. S. Barmina, and E. V. Kislov, "Petrology of Mafic–Ultramafic Layered Intrusions in Precambrian Platforms: State of the Problem and New Approaches," Geol. Geofiz. **44** (12), 1365–1373 (2003).
50. T. Wenzel, L. P. Baumgartner, G. E. Bruegman, et al., "Partial Melting and Assimilation of Dolomitic Xenoliths by Mafic Magma: the Ioko-Dovyren Intrusion (North Baikal Region, Russia)," J. Petrol. **43**, 2049–2074 (2002).
51. N. N. Pertsev, E. G. Konnikov, E. V. Kislov, et al., "Merwinite-Facies Magnesian Skarns in Xenoliths from Dunite of the Dovyren Layered Intrusion," Petrologiya **11**, 512–523 (2003) [Petrology **11**, 464–475 (2003)].
52. L. R. Wager and G. M. Brown, *Layered Igneous Rocks* (Oliver and Boyd, Edinburgh, 1967; Mir, Moscow, 1970).
53. Yu. V. Mironov, D. A. Ionov, G. S. Krivoplyasov, et al., "Structure of the Ioko–Dovyren Dunite–Troctolite–Gabbronorite Layered Massif (Northern Baikal Region)," Dokl. Akad. Nauk SSSR **250**, 1228–1232 (1980).
54. H. Papunen, V. Distler, and A. Sokolov, "PGE in the Upper Proterozoic Dovirensky Layered Complex, North Baikal Area, Siberia," Aust. J. Earth Sci. **39**, 327–334 (1992).
55. E. V. Kislov, "Silicate Enclaves in the Cr-Spinel of the Inner-Contact Dunites of the Ioko-Dovyren Massif," Geol. Geofiz., No. 10, 47–50 (1990).
56. A. A. Ariskin and A. A. Yaroshevskii, "Crystallization Differentiation of Intrusive Magmatic Melt: Development of a Convection–Accumulation Model," Geokhimiya, No. 1, 80–102 (2006) [Geochem. Int. **44**, 72–93 (2006)].
57. N. L. Bowen, *The Evolution of the Igneous Rocks* (Princeton Univ. Press, Princeton, New Jersey, 1928).
58. G. Chai and A. J. Naldrett, "The Jinchuan Ultramafic Intrusion—Cumulate of a High-Mg Basaltic Magma," J. Petrol. **33**, 277–303 (1992).
59. V. N. Sharapov, A. N. Cherepanov, V. N. Popov, and A. G. Lobov, "Dynamics of Basic Melt Cooling during the Filling of a Funnel-Shaped Intrusive Chamber," Petrologiya **5**, 10–22 (1997) [Petrology **5**, 8–19 (1997)].
60. M. Ya. Frenkel', *Thermal and Chemical Dynamics of the Differentiation of Basic Magmas* (Nauka, Moscow, 1995) [in Russian].
61. L. V. Danyushevsky, A. V. Sobolev, and L. V. Dmitriev, "Estimation of the Pressure of Crystallization and H_2O Content of MORB and BABB Glasses: Calibration of an Empirical Technique," Mineral. Petrol. **57**, 185–204 (1996).
62. R. R. Almeev, F. Holtz, J. Koepke, et al., "The Effect of H_2O on Olivine Crystallization in MORB: Experimental Calibration at 200 MPa," Am. Mineral. **92**, 670–674 (2007).

63. G. I. Marziano, F. Gaillard, and M. Pichavant, "Limestone Assimilation and the Origin of CO_2 Emissions at the Alban Hills (Central Italy): Constraints from Experimental Petrology," J. Volcanol. Geotherm. Res. **166**, 91–105 (2007).
64. E. V. Pushkarev and E. V. Kislov, "Chromites of the Yoko–Dovyren Massif (Northern Baikal Region) as Endoskarns in the Contaminated Dunites," in *Proceedings of International Conference on Ultramafic–Mafic Complexes of the Precambrian Folded Areas* (Izd-vo Buryatskogo NTs SO RAN., Ulan-Ude, 2005), pp. 89–93 [in Russian].
65. V. I. Ustinov, A. A. Yaroshevskii, V. A. Strizhov, et al., "Oxygen Isotopic Composition of Rock-Forming Minerals of the Yoko–Dovyren Dunite–Troctolite–Gabbro–Norite Massif (Northern Baikal Region)," in *Proceedings of 8th All-Union Symposium on Stable Isotopes in Geochemistry, Moscow, Russia, 1980* (Moscow, 1980), pp. 56–58 [in Russian].
66. G. S. Krivoplyasov, A. A. Yaroshevskii, and V. I. Ustinov, "Oxygen Isotopic Composition of the Rock-Forming Minerals and Some Differentiated Trap Sills and Large Layered Intrusions: An Example of Traps of the Norilsk District, Podkammennaya Tunguska River, and Yoko–Dovyren Massif," in *Proceedings of 10th All-Union Symposium on Stable Isotopes in Geochemistry, Moscow, Russia, 1984* (Moscow, 1984), p. 233 [in Russian].
67. J. Lehmann, N. Arndt, B. Windley, et al., "Field Relationships and Geochemical Constraints on the Emplacement of the Jinchuan Intrusion and Its Ni–Cu–PGE Sulfide Deposit, Gansu, China," Econ. Geol. **102**, 75–94 (2007).
68. J. M. Brenan and C. Li, "Constraints on Oxygen Fugacity during Sulfide Segregation in the Voisey's Bay Intrusion, Labrador, Canada," Econ. Geol. **95**, 901–915 (2000).
69. D. A. Orsoev, E. V. Kislov, and S. V. Kanakin, "Mineral Associations of Sulfides and Their Distribution in the Layered Series of the Yoko–Dovyren Massif. Geochemistry and Ore Formation of the Radioactive, Noble, and, and Rare Metals in Endogenic and Exogenic Processes," in *Proceedings of All-Russian Conference, Ulan-Ude, Russia, 2007* (BNTs SO RAN, Ulan-Ude, 2007), Part 2, pp. 66–71 [in Russian].
70. D. R. Houghton, P. L. Roeder, and B. J. Skinner, "Solubility of Sulfur in Mafic Magmas," Econ. Geol. **69**, 451–467 (1974).
71. H. St. C. O'Neill and J. A. Mavrogenes, "The Sulfide Capacity and the S Content at Sulfide Saturation of Silicate Melts at 1400°C and 1 bar," J. Petrol. **43**, 1049–1087 (2002).
72. L. N. Kacharovskaya, Extended Abstract of Candidate's Dissertation in Geology and Mineralogy (Ulan-Ude, 1986).
73. L. V. Danyushevsky, R. A. J. Leslie, A. J. Crawford, and P. Durance, "Melt Inclusions in Primitive Olivine Phenocrysts: The Role of Localised Reaction Processes in the Origin of Anomalous Compositions," J. Petrol. **45**, 2531–2553 (2004).
74. A. J. Naldrett, "Geological Settings Favorable for the Occurrence of Magmatic Sulfide Ores," Otech. Geol., No. 5, 33–47 (2002).
75. L. V. Danyushevsky, S. Sokolov, and T. J. Falloon, "Melt Inclusions in Olivine Phenocrysts: Using Diffusive Re-Equilibration to Determine the Cooling History of a Crystal, with Implications for the Origin of Olivine-Phyric Volcanic Rocks," J. Petrol. **43**, 1651–1671 (2002).
76. N. S. Rudashevskii, Yu. L. Kretser, D. A. Orsoev, and E. V. Kislov, "Palladium–Platinum Mineralization in Copper–Nickel Vein Ores in the Ioko–Dovyren Layered Massif," Dokl. Akad. Nauk **391**, 519–522 (2003) [Dokl. Earth Sci. **391**, 858–861 (2003)].
77. V. V. Distler and A. G. Stepin, "Low-Sulfide PGE-Bearing Unit of the Yoko–Dovyren Layered Ultrabasic–Basic Intrusion (Northern Baikal Region)," Dokl. Akad. Nauk **328**, 498–501 (1993).
78. E. V. Kislov and D. A. Orsoev, "Finding of Platinum-Group-Element-Bearing Horizons at the Ioko–Dovyren Layered Massif, Northern Transbaikalia," IAGOD, Newsletter, 23 (1993).
79. D. A. Orsoev, E. V. Kislov, E. G. Konnikov, et al., "Tendencies in the Distribution and Compositional Features of PGE Units of the Yoko–Dovyren Layered Massif (Northern Baikal Region)," Dokl. Akad. Nauk **340**, 225–228 (1995).
80. E. G. Konnikov, W. P. Meurer, S. S. Neruchev, et al., "Fluid Regime of Platinum Group Elements (PGE) and Gold-Bearing Reef Formation in the Dovyren Mafic–Ultramafic Layered Complex, Eastern Siberia, Russia," Miner. Deposita **35**, 526–532 (2000).
81. D. A. Orsoev, N. S. Rudashevskii, Yu. L. Kretser, and E. G. Konnikov, "Precious Metal Mineralization in Low-Sulfide Ores of the Ioko–Dovyren Layered Massif, Northern Baikal Region," Dokl. Akad. Nauk **390**, 233–237 (2003) [Dokl. Earth Sci. **390**, 545–549 (2003)].
82. A. I. Glotov, E. V. Kislov, D. A. Orsoev, et al., "Sulfur Isotope Geochemistry in Different Mineralization Types of the Yoko–Dovyren Massif (Northern Baikal Region)," Geol. Geofiz. **39** (2), 228–233 (1998).
83. E. G. Konnikov and E. V. Kislov, "Trends of Compositional Evolution of Ni-Bearing Complexes and Epochs of Cu–Ni–PGE Sulfide Ore Formation in the Precambrian," Dokl. Akad. Nauk **374**, 517–519 (2000) [Dokl. Earth Sci. **374**, 1100–1102 (2000)].
84. X. H. Li, L. Su, S.-L. Chung, et al., "Formation of the Jinchuan Ultramafic Intrusion and the World's Third Largest Ni–Cu Sulfide Deposit: Associated with the ~825 Ma South Chona Mafic Plume," Geochemistry, Geophysics, Geosystems **6** (11), 1–16 (2005).
85. Z. X. Li, D. A. D. Evans, and S. Zhang, "A 90° Spin on Rhodinia: Possible Causal Links Between the Neoproterozoic Supercontinent, Superplume, True Polar Wander and Low-Latitude Glaciation," Earth Planet. Sci. Lett. **220**, 409–421 (2004).
86. G. Chai and A. J. Naldrett, "Characteristics of Ni–Cu–PGE Mineralization and Genesis of the Jinchuan Deposit, Northwest China," Econ. Geol. **87**, 1475–1495 (1992).
87. N. L. Dobretsov and L. P. Zonenshain, "Comparison of the Riphean–Paleozoic Ophiolites of North Eurasia," in *Riphean–Lower Paleozoic Ophiolites of North Eurasia* (Nauka, Novosibirsk, 1985), pp. 181–190 [in Russian].

88. S. A. De Wall, Z. H. Xu, C. S. Li, and H. Mouri, "Emplacement of Viscous Mushes in the Jinchuan Ultramafic Intrusion, Western China," Can. Mineral. **42**, 371–392 (2004).
89. C. S. Li, Z. H. Xu, S. A. DeWaal, E. M. Ripley, and W. D. Maier, "Compositional Variations of Olivine from the Ni–Cu Sulfide Deposit, Western China: Implications for Ore Genesis," Miner. Deposita **39**, 159–172 (2004).
90. X.-Z. Yang, S. Ishihara, and H. Matsueda, "Multiphase Melt Inclusions in the Jinchuan Complex, China: Implications for Petrogenetic and Metallogenic Physico-Chemical Conditions," Int. Geol. Rev. **40**, 335–349 (1998).
91. M. F. Zhou, Z. X. Yang, and X. Y. Song, "Magmatic Ni–Cu–(PGE) Sulphide Deposits in China," in *The Geology, Geochemistry, Mineralogy, and Mineral Beneficiation of the Platinum-Group Elements*, Ed. by L.J. Cabri, Can. Inst. Mining. Metal. Petrol. **54** (Spec. Vol), 619–636 (2004)
92. N. F. Pchelintseva, A. V. Abramov, Yu. V. Mironov, et al., "Chalcophile Elements in the Yoko–Dovyren Layered Dunite–Troctolite–Gabbro–Norite Intrusion," Geokhimiya, No. 5, 608–619 (1985).
93. M. A. Nefed'ev, "Deep Structure and Estimate of the Prospects of the Dovyren Basic–Ultrabasic Massif Based on Geophysical Data (Northern Baikal Region)," in *Proceedings of International Conference on Ultramafic–Mafic Complexes of Precambrian Folded Areas, Ulan-Ude, Russia, 2005* (Buryatskii NTs SO RAN., Ulan-Ude, 2005), pp. 163–165 [in Russian].
94. R. F. Wendlandt, "Sulfide Saturation of Basalt and Andesite Melts at High Pressures and Temperatures," Am. Mineral. **67**, 877–885 (1982).
95. G. A. Gaetani and T. L. Grove, "Partitioning of Moderately Siderophile Elements among Olivine, Silicate Melt, and Sulfide Melt: Constraints on Core Formation in the Earth and Mars," Geochim. Cosmochim. Acta **61**, 1829–1846 (1997).
96. A. Holzheid and T. L. Grove, "Sulfur Saturation Limits in Silicate Melts and Their Implications for Core Formation Scenarios for Terrestrial Planets," Am. Mineral. **87**, 227–237 (2002).
97. J. A. Mavrogenes and H. St. C. O'Neill, "The Relative Effects of Pressure, Temperature and Oxygen Fugacity on the Solubility of Sulfide in Mafic Magmas," Geochim. Cosmochim. Acta **63**, 1173–1180 (1999).
98. P. G. Jugo, R. W. Luth, and J. P. Richards, "An Experimental Study of the Sulfur Content in Basaltic Melts Saturated with Immiscible Sulfide or Sulfate Liquids at 1300°C and 10 GPa," J. Petrol. **46**, 783–798 (2005).
99. C. Li and E. M. Ripley, "Empirical Equations to Predict the Sulfur Content of Mafic Magmas at Sulfide Saturation and Applications to Magmatic Sulfide Deposits," Miner. Deposita **40**, 218–230 (2005).
100. K. A. Bychkov, A. A. Ariskin, G. S. Barmina, and L. V. Danyushevsky, "A Test of Sulfide Solubility Models Using Anhydrous Experimental Melts and Natural Tholeiitic Glasses," in *Proceedings of 18th Annual Goldschmidt Conf. Vancouver, Canada, 2008," Geochim. Cosmochim. Acta* **72** (Suppl.), A126 (2008).
101. A. A. Ariskin, K. A. Bychkov, L. V. Danyushevsky, and G. S. Barmina, "A Model of S Solubility in Basaltic Melts at 1 atm," *Abstracts of 18th Annual Goldschmidt Conf. Vancouver, Canada*, 2008," Geochim. Cosmochim. Acta **72** (Suppl.), A31 (2008).
102. D. V. Lee, M. G. Muggridge, R. I. Wheeler, and D. H. C. Wilton, "Physical Controls Associated with the Distribution of Sulfides in the Voisey's Bay Ni–Cu–Co Deposit, Labrador," Econ. Geol. **95**, 749–769 (2000).
103. J. B. d'Ars, N. T. Arndt, and E. Hallot, "Analog Experimental Insights into the Formation of Magmatic Sulfide Deposits," Earth Planet. Sci. Lett. **186**, 371–381 (2001).
104. P. C. Lightfoot and A. J. Naldrett, "Geological and Geochemical Relationships in the Voiseyís Bay Intrusion, Nain Plutonic Suite, Labrador, Canada," Geol. Assoc. Can. Short. Course Notes **13**, 1–30 (1999).